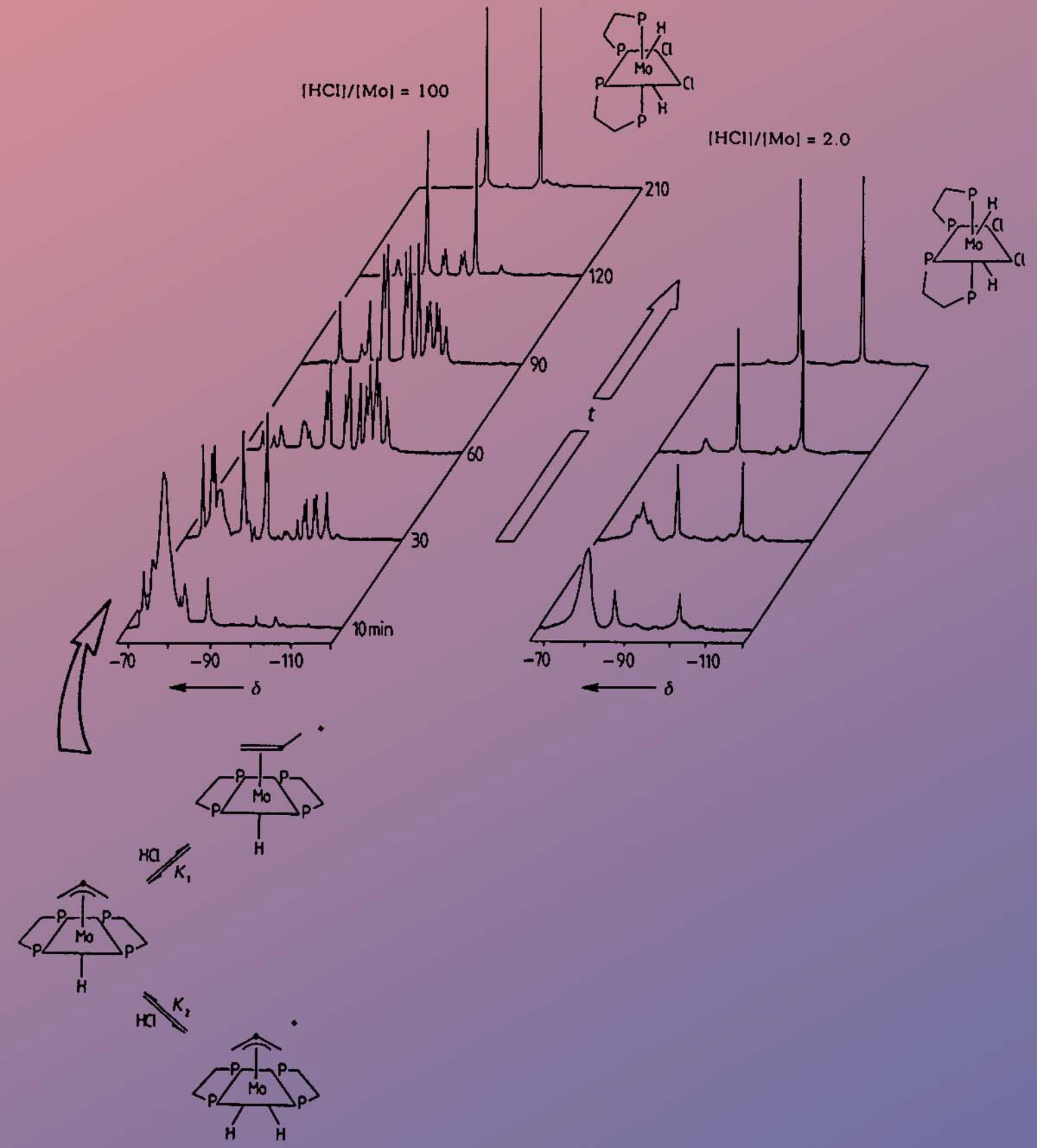

Intermediates in the protonation of a phosphane allyl molybdenum complex can be detected by ^{31}P NMR spectroscopy. For more about the kinetic analysis of protonation mechanisms for hydrocarbon transition metal complexes see the following article by R. A. Henderson.

Protonation of Unsaturated Hydrocarbon Ligands: Regioselectivity, Stereoselectivity, and Product Specificity

Richard A. Henderson*

Understanding the mechanisms of protonation of hydrocarbon ligands is fundamental to a wide range of chemistry including organic synthesis, organometallic chemistry, and even bioinorganic chemistry. Protonation at carbon or metal sites is often slow, with the result that in species containing both types of sites, initial protonation can be at either the metal or the carbon. This has fundamental consequences on the reactivity of hydrocarbon ligands, which are highlighted in this article. In particular, many reactions are apparently the result of a regioselective protonation on the basis of structural analysis of the isolated products. In fact, these products are often formed by an indirect route involving kinetically controlled protonation at the "wrong" site followed by rearrangement to form the thermodynamically controlled, apparently regioselective, product. Other aspects of the protonation mechanisms of complexes containing hydrocarbon ligands are discussed, with an emphasis on the manner in which competitive protonation at metal or ligand can be exploited to select which hydrocarbon is produced and to control the stereochemistry of the hydrocarbon.

Keywords: complexes with carbon ligands · hydrocarbons · protonation · reaction mechanisms

1. Introduction

The binding and activation of small molecules at metal sites is an area of research which is of interest to a wide range of chemists—from those involved in the simple stoichiometric reactions of inorganic compounds to those defining the elementary reactions of organometallic homogeneous catalysts, metalloenzymes, and even heterogeneous catalysts. In this article I will concentrate on the protonation of small, unsaturated hydrocarbon residues bound to relatively simple, electron-rich transition metal sites.

The chemistry of carbon residues bound to metal sites has traditionally been considered the domain of organometallic chemists; however, for many years (since the discovery of the cobalt–carbon bond in the vitamin B_{12} coenzyme)[1] it has been appreciated that bioinorganic chemistry can have an organometallic flavor.[2] Clearly in the vitamin B_{12} case, the connection between organometallic and bioinorganic chemistry is based on a structural feature. However, if some of the elementary reactions of metalloenzymes are considered, then further aspects common to organometallic and bioinorganic chemistry become evident. Examples are the 1,2-shifts associated with several types of enzymes, which are initiated by homolysis of the cobalt–carbon bond in the vitamin B_{12} coenzyme;[3] the reduction of carbon dioxide to methane by dihydrogen in methanogenic and acetogenic bacteria containing carbon monoxide dehydrogenase (in anaerobic bacteria a nickel-containing enzyme and in aerobic bacteria a molybdopterin enzyme);[4] and the mono- or dioxygenation of organic molecules by methane monoxygenase[5] and catecholases[6] (iron-containing enzymes). All involve the reaction, or intermediacy, of species containing metal–carbon bonds.

A family of enzymes that are of particular interest (at least to the author!) are the nitrogenases. These enzymes contain iron together with molybdenum or vanadium and transform dinitrogen into ammonia with the concomitant release of some dihydrogen in vivo [Eq. (1)].[7] In vitro the enzyme is capable of

$$N_2 + 8H^+ + 8e^- \longrightarrow 2NH_3 + H_2 \quad (1)$$

transforming a wide range of other small, unsaturated molecules by a sequence of electron and proton transfer reactions. The range of alternative substrates include acetylenes, cyclopropenes, azides, isonitriles, and cyanides. It is worth noting that in several of these a metal–carbon bond must be formed upon binding of the substrate. Of these substrates, the reactions of the nitrogenases with acetylene to form ethene and ethane [Eqs. (2) and (3)], respectively, warrant further comment.

$$C_2H_2 + 2H^+ + 2e^- \longrightarrow C_2H_4 \quad (2)$$

$$C_2H_2 + 4H^+ + 4e^- \longrightarrow C_2H_6 \quad (3)$$

The nitrogenases exhibit a different product specificity in their reactions with acetylene. The molybdenum-based nitroge-

[*] Dr. R. Henderson
John Innes Centre, Nitrogen Fixation Laboratory
University of Sussex, Brighton BN1 9RQ (UK)
Present address: Nitrogen Fixation Laboratory, John Innes Centre
Norwich Research Park, Colney, Norwich (UK)

nase converts acetylene into ethene exclusively, whilst the vanadium-based enzyme gives predominantly ethene but also some ethane (about 5%). In addition, both nitrogenases exhibit a stereoselectivity in their reactions with acetylene. In the presence of D_2O both enzymes give *cis*-CHDCHD as the exclusive product. The manner in which the enzyme accomplishes such stereoselectivity and product specificity by simple electron and proton transfer reactions was the inspiration of much of our own work in this area.

In this article we shall see that the fundamental mechanistic chemistry associated with the protonation of hydrocarbon residues bound to a transition metal center is a consequence of slow protonation at both metal and carbon sites. Only by understanding the basic mechanistic principles associated with protonation of simple complexes containing hydrocarbon residues can we appreciate how to harness this reactivity to accomplish stereoselective or product-specific reactions.

2. General Considerations on the Rates of Protonation

Throughout this article we shall be concerned with the protonation of unsaturated carbon residues bound to metal sites; consequently it is pertinent to start with a short, entirely general, discussion of the factors that influence the rates of protonation at various sites. This will necessarily be a "broad brush strokes" approach, and the interested reader is referred to specialist reviews of this area for a more detailed discussion.[8–10]

2.1. Rates of Proton Transfer

In general, for the simple process described by Equation (4) there is no chemical barrier for thermodynamically favorable reactions involving attachment of the proton to bases at an O,

$$H^+ + X^- \rightleftharpoons HX \tag{4}$$

N, F, or S site. The rate of the reaction is restricted only by the rate at which the two components diffuse together ($k_{diff} \approx 1 \times 10^{10}\ dm^3\,mol^{-1}\,s^{-1}$). The rate of the reverse reaction is necessarily smaller by a factor dependent on the thermodynamic driving force of the reaction, K_a, (that is, $10^{\Delta pK_a}$). If the forward reaction is not thermodynamically favorable, the rate of the reaction is dependent on the thermodynamic driving force, as given by the Brønsted relationship in Equation (5),

$$k = G_a K_a^{\alpha} \tag{5}$$

where G_a and α are constants. Thus, for the protonation of a series of structurally analogous bases, the curve of the plot of $\log k$ against $\log K_a$ initially has a slope of unity under conditions where the proton transfer is thermodynamically uphill, but levels off to a slope of zero when the proton transfer is thermodynamically favorable.

Exceptions to this general rule occur when there is a considerable change in the structure of the O, N, F, or S acid or base upon proton transfer, and then the rate is slower than the diffusion-controlled limit. For instance, the deprotonation reaction in Equation (6) is a thermodynamically favorable reaction, but

$$^-O_2NNCH_2CH_2NHNO_2 + NH_3 \rightleftharpoons {}^-O_2NNCH_2CH_2NNO_2^- + NH_4^+ \tag{6}$$

the forward rate constant ($k \approx 10^5\ dm^3\,mol^{-1}\,s^{-1}$) is five orders of magnitude slower than the diffusion-controlled limit.[11] This relatively slow rate of proton transfer indicates that there is a significant barrier to removal of the proton from the monoanionic species, which is probably associated with the delocalization of the lone pair of electrons over the NNO_2 residue.

2.2. Proton Transfer at Carbon Sites

We can consider the deprotonation of the CH_2NO_2 residue in nitroethane, as shown in Equation (7), to be the carbon ana-

$$MeCH_2NO_2 + NH_3 \rightleftharpoons MeCHNO_2^- + NH_4^+ \tag{7}$$

logue of the reaction in Equation (6).[12] The rate of this deprotonation is $k = 7 \times 10^{-3}\ dm^3\,mol^{-1}\,s^{-1}$. This example illustrates an entirely general principle: deprotonation of a carbon residue is markedly slower than deprotonation of the "analogous" nitrogen-based residue. This difference between the normal behavior exhibited by O, N, F, or S sites and carbon

Born in 1951 just outside London, Richard A. Henderson studied chemistry at University College London, receiving his PhD in 1976 under the supervision of Martin L. Tobe. After two years as postdoctoral fellow with A. Geoffrey Sykes at the University of Leeds, he moved to the Nitrogen Fixation Laboratory at the University of Sussex in October 1979. His major research interests are in mechanistic inorganic chemistry, in particular the binding of small molecules such as N_2, H_2, RNC, RCN, or unsaturated hydrocarbons to transition metal sites, and their activation towards protonation. More recently his interests have extended to the mechanisms of the reactions of iron–sulfur-based clusters. In 1993 he was the first recipient of the Royal Society of Chemistry Award in Inorganic Reaction Mechanisms.

sites is further emphasized by comparing the rates of the proton transfer reactions shown in Equations (8) and (9).[13]

$$MeCH_2NO_2 + OH \rightleftharpoons MeCHNO_2^- + H_2O \quad (8)$$

$$C_6H_5OH + OH \rightleftharpoons C_6H_5O^- + H_2O \quad (9)$$

Although phenol is a weaker acid than nitroethane, and consequently the thermodynamic driving force is larger for reaction (8), the rate of deprotonation of phenol is diffusion-controlled ($k = 1.5 \times 10^{10}\ dm^3 mol^{-1} s^{-1}$), whereas the deprotonation of nitroethane is much slower ($k = 5.2\ dm^3 mol^{-1} s^{-1}$).

There are two reasons why the rates of proton transfer involving carbon sites are slow. First, with O, N, F, or S sites, proton transfer is preceded by the formation of a hydrogen bond between the sites involved in the proton transfer, and this anchoring of the two sites facilitates the subsequent transfer of the proton. Such hydrogen bonding is much weaker in the case of carbon-based residues. Second, carbon is weakly electronegative, and thus lone pairs of electrons on a carbon atom become delocalized towards more electronegative neighboring atoms. This delocalization involves a change in the electronic structure and in the position of all the nuclei involved, and consequently results in a slow rate of proton transfer.

Clearly, if electronic and structural reorganization factors become less important in the reactions of carbon-based sites the rates of proton transfer can become fast. Thus, in the deprotonation of cyano or disulfano compounds,[14] the rates of proton transfer for thermodynamically favorable reactions are $k \approx 10^7$–$10^8\ dm^3 mol^{-1} s^{-1}$. Although these rates are still at least 100 times less than the normal diffusion-controlled limit, they are significantly faster than those normally observed with carbon-based residues. The rapidity of these reactions indicate that after deprotonation of the conjugate acid the lone pair of electrons resides predominantly on the carbon, rather than being delocalized.

2.3. Proton Transfer at Metal Sites

In general, proton transfer to and from metal sites is slow.[10, 15] The origin of this slowness is associated with the significant electronic and structural reorganization that must occur at the metal upon proton transfer. In an extensive series of studies on the rates of deprotonation of hydridic complexes by aniline, a range of reactions exhibiting a variety of thermodynamic driving forces (from exothermic to endothermic) have been studied, and a variety of rate constants have been observed: $[CoH(CO)_4]$ ($k = 1.7 \times 10^6\ dm^3 mol^{-1} s^{-1}$, $\Delta pK_a = -2.3$); $[FeH_2(CO)_4]$ ($k = 5.4 \times 10^4\ dm^3 mol^{-1} s^{-1}$, $\Delta pK_a = +0.8$); and $[OsH_2(CO)_4]$ ($k = 1.0 \times 10^{-2}\ dm^3 mol^{-1} s^{-1}$; $\Delta pK_a = +10.2$).[16] There are two features to note that are typical of proton transfer reactions at metals: first, the rates vary with the thermodynamic driving force of the reaction, and second, the rates never attain the diffusion-controlled limit.

In summary then, although the rates of protonation are usually defined by the rate of diffusion of the two components (the acid and the base), two notable exceptions are the protonation of carbon sites and the protonation of metal sites. Consequently, the difference in the rates of protonation of the ligand and the metal in the complexes containing hydrocarbon ligands may be rather small, and, depending on the system under investigation, either the metal or the hydrocarbon can be the more rapidly protonated site.

3. Regioselective Protonation of Complexes

On studying the protonation of unsaturated carbon-based residues bound to metal sites the first pertinent question, in the light of the discussion above, is, "Which site is protonated first: metal or carbon?" This is a question that cannot always be answered by synthetic chemistry. Merely to isolate the product from the reaction of an acid with any particular complex will often result in the identification of the thermodynamically controlled product. What we want to identify is the *initial* site of protonation: the kinetically controlled product. Only if the interconversion of the kinetically controlled and thermodynamically controlled products is slow will it be possible to identify the true initial site of protonation by synthetic chemistry. In order to establish unambiguously which site is protonated first, the reaction must be monitored by a sufficiently rapid method. The most commonly used technique is stopped-flow spectrophotometry, which can study reactions that take longer than about two milliseconds to complete. More conventional, and diagnostic, spectroscopy such as solution IR and multinuclear NMR spectroscopies can be used, but often low temperatures must be employed to slow these reactions sufficiently and ensure that no intermediates have avoided detection.

Protonation at the metal and the hydrocarbon can be completely isolated processes. For instance, the reaction of acids with $[Ru(\eta^5\text{-}C_5H_5)_2]$ results in protonation of the metal as shown in Scheme 1. However, at the same time, H–D exchange of the cyclopentadienyl protons occurs indicating protonation of the hydrocarbon ligands.[17] As the protonation of the metal becomes more extensive (for instance, when stronger acids or higher concentrations of acid are used), the extent of H–D exchange of the ring protons decreases. That is, protonation of the metal and hydrocarbon are competitive processes, and protonation at the metal deactivates the cyclopentadienyl ring towards protonation.

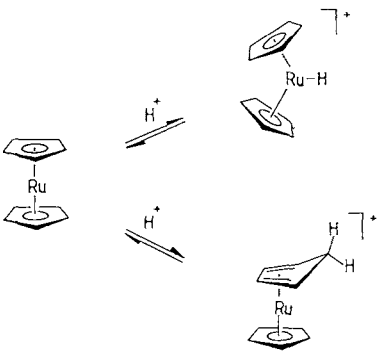

Scheme 1. The reaction of acids with $[Ru(\eta^5\text{-}C_5H_5)_2]$

However, a more common situation is that protonation at the metal or the hydrocarbon residue are not mutually independent, because of facile pathways that can transfer the proton from the metal to the carbon. This leads to another pertinent question: "What is meant by a regioselective protonation?" If we consider just the stoichiometry of the reaction and the structure of the product, then (for instance) the conversion of an alkylidyne into an alkylidene, as shown in Scheme 2, is a regioselec-

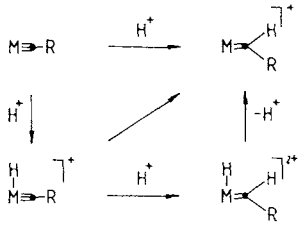

Scheme 2. The protonation of alkylidyne complexes.

tive protonation. However, if we consider the reaction mechanistically, this apparent regioselectivity could result by three pathways: direct protonation of the carbon atom, protonation of the metal followed by intramolecular migration to the carbon, or protonation of the metal followed by an acid–base catalyzed rearrangement.

We shall see in the examples that follow in this article that true regioselective protonation is rare, and initial protonation at the "wrong" site still allows formation of the product by intramolecular or acid–base catalyzed pathways. We shall also see that no generalization can be made about which site (metal or hydrocarbon) is protonated first. It appears that the energetic barriers to protonation at the metal and a coordinated carbon are rather similar, and which is protonated the faster cannot be defined a priori. In the remainder of this section we shall consider some simple stoichiometric reactions, which together illustrate the sequence of elementary reactions shown in Scheme 3.

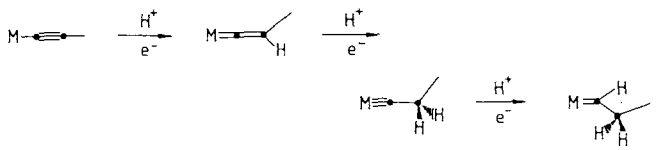

Scheme 3. A typical protonation of an alkynyl ligand to form a vinylidene.

This sequence has been chosen because each step it contains is stoichiometrically very simple, involving the addition of only a single proton, and consideration of the structure of the product would indicate the regioselective addition of a proton. However, studies on each step demonstrate that the interconversions are often mechanistically more complicated, less direct, and certainly less obvious. These studies demonstrate some useful mechanistic principles upon which we shall build in later sections.

The addition of a proton directly to its final residence, whether it be the metal or the carbon, exhibits a simple first-order dependence on the concentration of the acid. In the mechanistic studies that follow, two features are diagnostic of a more complicated mechanism: 1) a complicated rate law, and in particular a complicated dependence on the concentration of acid, and 2) the spectroscopic detection of an intermediate, the kinetically controlled product.

3.1. Protonation of an Alkynyl Ligand to a Vinylidene

This common reaction[18] is typified by the reaction of PhCCH with *fac*-[W(thf)(CO)$_3$(dppe)] (dppe = $Ph_2PCH_2CH_2PPh_2$; thf = C_4H_8O)[19] shown in Scheme 4. After the initial binding of the alkyne to the metal, rearrangement to the isomeric vinylidene complex occurs when the solution is warmed to 50 °C. Despite the prevalence of this transformation, the mechanism has not been studied in detail. However, molecular orbital calculations suggest that because of the importance

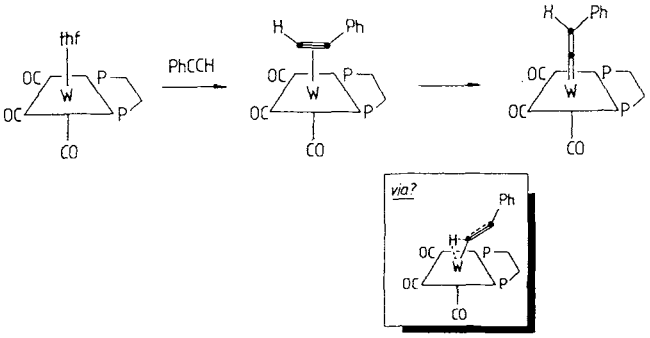

Scheme 4. Binding of PhCCH to *fac*-[W(thf)(CO)$_3$(dppe)] and rearrangement to the vinylidene complex.

of π donation from the alkyne, the rearrangement to form the vinylidene is promoted by the unfavorable four-electron, two-center bonding between the alkyne π orbitals and the filled metal d orbitals. Equally, the π complex might rearrange, because the carbon monoxide coligands render the coordinated PhCCH sufficiently acidic for the proton to be released with concomitant formation of the alkynyl species. Subsequent protonation of the alkynyl ligand at the carbon atom remote from the metal generates the vinylidene complex. Certainly, protonation of isolated alkynyl complexes gives vinylidene species, and this reaction has been studied mechanistically.

The rate of protonation of [Ru(η^5-C_5H_5)(CCMe)(PMe_3)$_2$] by [W(η^5-C_5H_5)H(CO)$_3$] shown in Equation (10)[20] is only ten

$$[Ru(\eta^5\text{-}C_5H_5)(CCMe)(PMe_3)_2] + [W(\eta^5\text{-}C_5H_5)H(CO)_3] \longrightarrow [Ru(\eta^5\text{-}C_5H_5)(CCHMe)(PMe_3)_2]^+ + [W(\eta^5\text{-}C_5H_5)H(CO)_3]^- \quad (10)$$

times faster than the rate of proton transfer from this hydrido complex to $PhNH_2$, although the alkynyl to vinylidene reaction is thermodynamically favorable by 1.5 kJ mol^{-1}, whilst the proton transfer to $PhNH_2$ is unfavorable by 1.8 kJ mol^{-1}. This relatively small difference in the rates of proton transfer indicates that, in general, the protonation of the alkynyl complex involves substantial structural and electronic reorganization.

Mulliken population analysis from molecular orbital calculations indicates that the gross atomic charge at the carbon atom remote from the metal is not significantly different for alkynyl and corresponding vinylidene species.[21] Consequently, if protonation of the alkynyl is charge-controlled and occurs at the remote carbon atom, it could be argued that protonation of the vinylidene would also occur at the remote carbon atom to form the alkylidyne. As we shall see in the next example, it is not this simple.

3.2. Protonation of a Vinylidene Ligand to an Alkylidyne

Protonation of vinylidene complexes invariably gives the corresponding alkylidyne in an apparently regioselective protonation of the remote carbon atom.[22] However, mechanistic studies on the reaction of the rhenium complex[23, 24] [Eq. (11)]

$$trans\text{-}[ReCl(CCHPh)(dppe)_2] + NHEt_3^+ \longrightarrow trans\text{-}[ReCl(CCH_2Ph)(dppe)_2]^+ + NEt_3 \quad (11)$$

demonstrate that this transformation can occur by three pathways (Scheme 5).

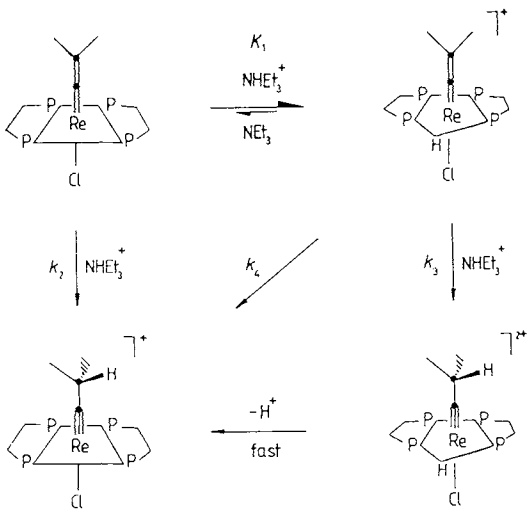

Scheme 5. Three potential pathways for the protonation of a vinylidene complex to the corresponding alkylidyne complex.

Consideration of this mechanism, assuming that k_2, k_3, and k_4 are the rate-limiting steps and that K_1 is a rapidly established protonation equilibrium, demonstrates that the rate law for the formation of the alkylidyne product is given by Equation (12).

$$k_{obs} = \frac{k_4K_1[NHEt_3^+]/[NEt_3] + (k_3K_1[NHEt_3^+]/[NEt_3] + k_2)[NHEt_3^+]}{1 + K_1[NHEt_3^+]/[NEt_3]} \quad (12)$$

Clearly, the complex acid dependence associated with this mechanism is readily distinguished from the simple first-order dependence on the concentration of acid expected for a direct protonation of the remote carbon site.

The most important feature of this mechanism is that direct, regioselective protonation of the vinylidene ligand (k_2) is slow, whilst protonation at another site, probably the metal (K_1), is rapid. It is important to emphasize that the formation of this hydride is enforced because of the difference in the rates of protonation of the carbon and metal sites. Chemical intuition tells us that this protonation must deactivate the vinylidene towards protonation by decreasing the electron density at the ligand. Nevertheless, formation of the alkylidyne subsequently occurs by both an intramolecular (k_4) and an acid-catalyzed (k_3) pathway .

In experiments with no added NEt_3, the equilibrium K_1 lies far to the right-hand side ($K_1[NHEt_3^+]/[NEt_3] \gg 1$), and the rate law is given by Equation (13). Under these conditions,

$$k_{obs} = k_4 + k_3[NHEt_3^+] \quad (13)$$

a linear dependence on the concentration of acid is observed, with a finite intercept, and the initial absorbance of the absorbance–time curve is distinctly different from that expected of *trans*-[ReCl(CCHPh)(dppe)$_2$], corresponding to the formation of the hydride within the dead time of the stopped-flow apparatus. Analysis of the data gives $k_4 = 7.3 \times 10^{-2}\,s^{-1}$, $k_4^H/k_4^D = 1.16$, and $k_3 = 9.4\,dm^3\,mol^{-1}\,s^{-1}$, $k_3^H/k_3^D = 1.35$. The acid-independent term in the rate law is associated with an intramolecular migration of the hydride ligand to the remote carbon atom. The isotope effect associated with this pathway is a consequence of the rate-limiting movement of a hydride (deuteride) whose origins are the addition of a proton (deuteron) to the metal.

In the presence of an excess of NEt_3 the position of the equilibrium, K_1, lies to the left-hand side. Consequently, $K_1[NHEt_3^+]/[NEt_3] \ll 1$, and the rate law reduces to that shown in Equation (14). From analysis of the data collected

$$k_{obs} = k_4 + \{k_3 + k_2[NEt_3]\,K_1[NHEt_3^+]\}[NHEt_3^+] \quad (14)$$

under these conditions and using the previously determined value of k_4, we can calculate, $k_2/K_1 = 17.6\,dm^3\,mol^{-1}\,s^{-1}$ and $k_3 = 10.5\,dm^3\,mol^{-1}\,s^{-1}$. Furthermore, since we can estimate that K_1 is greater than 4, k_2 is larger than $70.4\,dm^3\,mol^{-1}\,s^{-1}$. The values of k_2 and k_3 both correspond to the protonation of the vinylidene ligand, but the much lower value of k_3 (corresponding to the protonation of the vinylidene ligand in *trans*-[Re(H)Cl(CCHPh)(dppe)$_2$]$^+$) confirms the earlier intuitive conclusion that initial protonation at the metal decreases the basicity of the hydrocarbon residue.

The formation of the alkylidyne complex is associated with a strong thermodynamic driving force, but kinetic factors initially result in the protonation of the "wrong" site—the rhenium center. Subsequently the complex transfers the proton from the metal to the carbon atom by both an acid-catalyzed rearrangement and a pathway (k_4) that appears to be intramolecular. Although the details of the intramolecular route have yet to be defined, it seems unlikely that the proton just "hops" from metal to the remote carbon atom. A more likely mechanism involves rate-limiting intramolecular migration to form a vinyl species, which subsequently protonates to form the corresponding alkylidene (Scheme 6). Subsequent proton loss from the carbon adjacent to the metal produces the alkylidyne complex. This type of acid-catalyzed rearrangement of vinyl species has been observed in the reactions of *trans*-[Mo(η^2-MeCCH)$_2$(dppe)$_2$] (see Section 4.1).

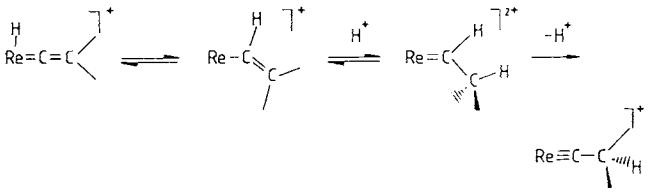

Scheme 6. Proposed mechanism for the intramolecular hydrogen transfer from the metal center to the remote carbon atom of the vinylidene complex, *trans*-[Re(H)Cl(CCHPh)(dppe)$_2$]$^+$.

In discussing this example I have stressed the details of the absorbance–time traces. The importance of establishing that the absorbance change being monitored is that expected for the reaction in question cannot be overemphasized. In addition, the observation that the initial absorbance is different from that of the reactant is indicative of the rapid formation of an intermediate. Even if the initial absorbance change had not been noticed (or, as happens in other systems, is much less marked) the experimenter would be alerted to something having occurred within the dead time of the apparatus by the kinetics of the subsequent step. An acid-independent pathway is very difficult to rationalize in such a stoichiometrically simple protonation reaction!

3.3. Protonation of an Alkylidyne Ligand to an Alkylidene

Protonation of alkylidyne complexes can occur at either the metal or the carbon atom bound to the metal, and the factors that distinguish between protonation of the two sites are rather subtle.[25] For instance, protonation of $[W(CH)L_4Cl]$ gives the hydride $[WH(CH)L_4Cl]^+$ when L_2 is $Me_2PCH_2CH_2PMe_2$ and the alkylidene $[W(CH_2)L_4Cl]^+$ when L is PMe_3.

Molecular orbital calculations[26] indicate that the HOMO in alkylidyne complexes may be metal-centered or ligand-centered, or it may be the orbital of the metal–carbon π bond. Calculations of this type also indicate that the alkylidyne residue is always negatively charged, and in particular for the fragment $MoCCH_2tBu$, the build-up of charge is at the carbon atom adjacent to the metal. If the protonation of this residue is frontier orbital controlled, then attack is at the metal (where the HOMO is centered), whereas if the protonation is charge-controlled, attack is at the carbon.[27] Studies on $[Mo(\eta^5\text{-}C_5H_5)(CCH_2tBu)\{P(OMe)_3\}_2]$ indicate that protonation is charge-controlled; the initial site of attack is the carbon atom, and subsequent formation of the hydrido species occurs by an intramolecular hydrogen shift from the alkylidene group as shown in Scheme 7. Studies on $[W(CPh)(CNtBu)Cl(CO)(PMe_3)_2]$, in

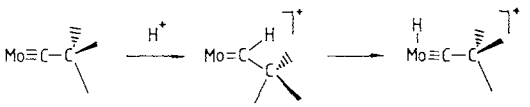

Scheme 7. Proposed mechanism for the protonation of $[Mo(\eta^5\text{-}C_5H_5)(CCH_2tBu)\{P(OMe)_3\}_2]$.

which three sites (metal, isocyanide, or alkylidyne) are potentially protonatable, indicates that the alkylidyne is protonated preferentially.[28]

It is worth noting that some alkylidene complexes can undergo rearrangement into the corresponding alkene, and in certain cases this process has been shown to be acid-catalyzed (Scheme 8).[29] The mechanism presumably involves the forma-

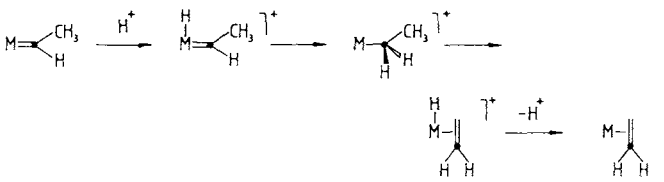

Scheme 8. Acid-catalyzed rearrangement of an alkylidene complex to form an alkene complex.

tion of a transient alkyl species, which then undergoes an intramolecular hydrogen migration from the remote carbon atom (β-hydrogen transfer) and subsequent proton release. However such rearrangements are not always acid catalyzed, as for example the intramolecular conversion of $[Re(\eta^5\text{-}C_5H_5)(CHEt)(NO)(PPh_3)]$ into $[Re(\eta^5\text{-}C_5H_5)(\eta^2\text{-}MeCHCH_2)(NO)(PPh_3)]$.[30]

There are two other examples in which apparent regioselective protonation occurs, but mechanistic studies demonstrate that the pathway is complicated. These examples will be discussed in this section, although they do not fall into any of the above headings.

3.4. Protonation of *trans*-$[\overline{Re(CH_2CCPh)Cl(dppe)_2}]$

The reaction of anhydrous HCl with the substituted coordinated allene complex, *trans*-$[\overline{Re(CH_2CCPh)Cl(dppe)_2}]$ gives an η^2-vinyl species in an apparently regioselective protonation as described by Equation (15).[31,32] This reaction exhibits a

$$trans\text{-}[\overline{Re(CH_2CCPh)Cl(dppe)_2}] + HCl \longrightarrow trans\text{-}[\overline{Re(\eta^2\text{-}CH_2CCHPh)Cl(dppe)_2}]^+ + Cl^- \quad (15)$$

simple first-order dependence on the concentration of the complex but a complicated dependence on the concentration of HCl as shown in Figure 1.[33] The complexity of this acid dependence

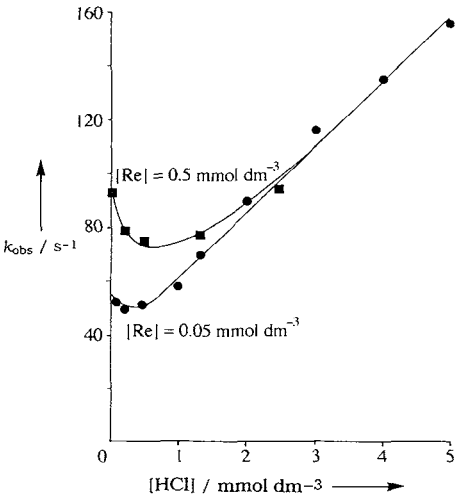

Fig. 1. Dependence of the observed rate constant k_{obs} on acid concentration for the protonation of *trans*-$[\overline{Re(CH_2CCPh)Cl(dppe)_2}]$.

is clearly inconsistent with any trivial mechanism involving direct protonation at the phenyl-substituted carbon atom, but is consistent with the mechanism shown in Scheme 9, in which the first step is the protonation of the metal ($K_1 > 80$; $k_1 \geq 1 \times 10^6\ dm^3\ mol^{-1}\ s^{-1}$) to give the hydrido species

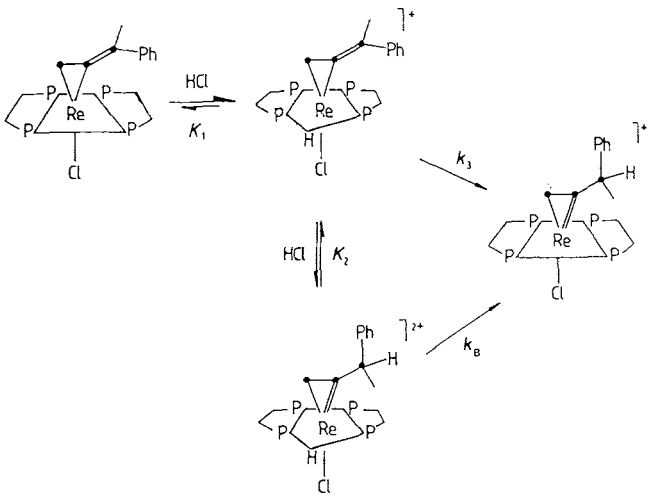

Scheme 9. Proposed mechanism of the protonation of *trans*-$[\overline{Re(CH_2CCPh)Cl(dppe)_2}]$.

$[\overline{Re(CH_2CCPh)}(H)Cl(dppe)_2]^+$, which occurs within the dead time of the stopped-flow apparatus (2 ms). This protonation would appear to be frontier orbital controlled, since extended Hückel calculations[32] indicate that the HOMO of *trans*-$[\overline{Re(CH_2CCPh)}Cl(dppe)_2]$ comprises predominantly the d_{xy}/d_{yz} orbitals on the rhenium atom (54%); the remaining electron density is divided between the phenyl-substituted carbon (36%) and the unsubstituted carbon atoms (10%) of the double bond.

The addition of the proton, albeit at the metal rather than the carbon, means that the stoichiometric requirements of reaction (15) have been met. The subsequent formation of the η^2-vinyl complex is associated with the rate law shown in Equation (16). This rate law describes two pathways: an intramolec-

$$k_{obs} = \{k_3 + K_2[HCl]/[Cl^-]\sum_B k_B[B]\}/(1 + K_2[HCl]/[Cl^-]) \quad (16)$$

ular route ($k_3 = 94\ s^{-1}$) and an acid–base catalyzed route. The latter pathway involves rapid protonation of the hydrido complex ($K_2 = 1.37\ dm^3\ mol^{-1}$), followed by rate-limiting deprotonation of the metal by any base present in the system (k_B). The bases present in the system are the solvent (THF: $k_{THF} = 2.7\ dm^3\ mol^{-1}\ s^{-1}$), Cl^- ($k_{Cl} = 2.4 \times 10^4\ dm^3\ mol^{-1}\ s^{-1}$), and even the chloro group in HCl ($k_{HCl} = 3.4 \times 10^4\ dm^3\ mol^{-1}\ s^{-1}$).

The intramolecular pathway may be a direct, intramolecular transfer of the hydrogen from the metal to the carbon terminus. Consideration of the X-ray crystal structure of *trans*-$[\overline{Re(CH_2CCPh)}Cl(dppe)_2]$ indicates that in the intermediate $[\overline{Re(CH_2CCPh)}(H)Cl(dppe)_2]^+$ the hydrido ligand may be no more than 1.5–1.8 Å from the phenyl-substituted carbon atom—sufficiently close to permit a reasonably facile transfer.

3.5. Protonation of *trans*-$[W(\eta^2\text{-}C_2H_4)_2(dppe)_2]$

The reaction of an excess of anhydrous HX (X = Cl or Br) with *trans*-$[W(\eta^2\text{-}C_2H_4)_2(dppe)_2]$ gives the pentagonal-bipyramidal hydrido species shown in Equation (17).[34] Protonation

$$trans\text{-}[W(\eta^2\text{-}C_2H_4)_2(dppe)_2] + HX \longrightarrow [WH(\eta^2\text{-}C_2H_4)_2(dppe)_2]^+ + X^- \quad (17)$$

would appear to involve regioselective attack at the metal center. When studied on a stopped-flow spectrophotometer, the reaction clearly occurs in two distinct phases. Typical absorbance–time traces for this reaction, at high and low concentrations of acid, are shown in Figure 2. At all acid concentrations the curves are exponential, and at low concentrations of acid the initial absorbance is that of *trans*-$[W(\eta^2\text{-}C_2H_4)_2(dppe)_2]$, and the final absorbance is that of the hydride product. However, at higher concentrations of acid, although the final absorbance still corresponds to that of the hydride, the initial absorbance is now markedly lower than that of the parent complex, and at intermediate acid concentrations intermediate initial absorbances are observed. The dependence of the initial absorbance on the concentration of HX can be quantified as shown on the left-hand side of Figure 2: this analysis demonstrates that within 2 ms an equilibrium associated with the addition of a single proton to *trans*-$[W(\eta^2\text{-}C_2H_4)_2(dppe)_2]$ is established. However, this proton must have been added to the wrong position, since a further reaction (associated with the exponential decay) is required to form the hydride.

The subsequent formation of the hydrido product occurs by two pathways: one acid-independent and another showing a first-order dependence on the concentration of acid. All of this behavior is consistent with the mechanism shown in Scheme 10.

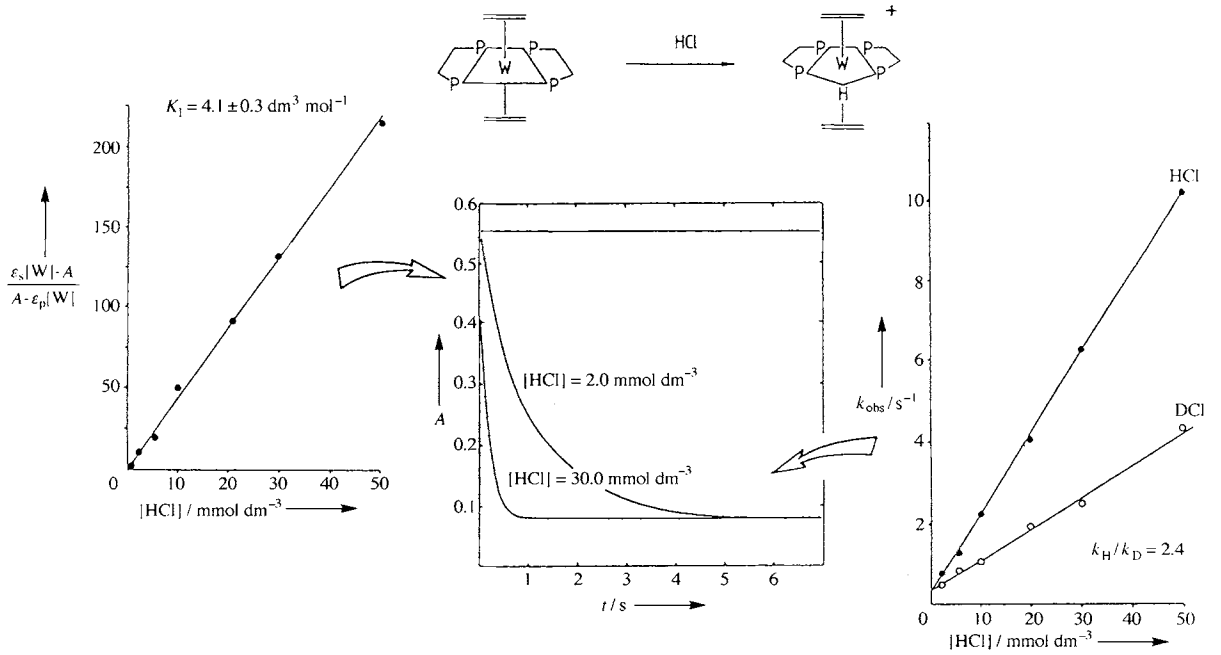

Fig. 2. The protonation of *trans*-$[W(\eta^2\text{-}C_2H_4)_2(dppe)_2]$ (top) and the experimental absorbance–time traces (bottom center). The dependence of the initial absorbance on acid concentration is depicted on the left (ε_s: extinction coefficient of the starting material, ε_p: extinction coefficient of the product, [W]: total tungsten concentration) and the plots of the observed rate constant k_{obs} against acid concentration for HCl and DCl on the right.

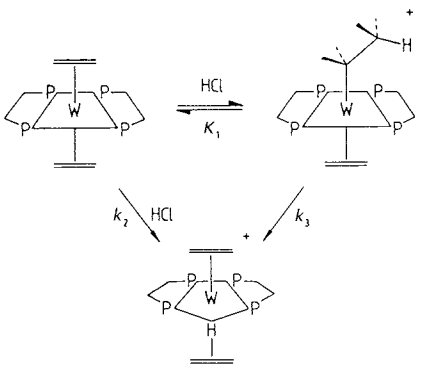

Scheme 10. Proposed mechanism for the protonation of *trans*-[W(η^2-C_2H_4)$_2$(dppe)$_2$].

Thus in a rapid equilibrium the ethene ligand is protonated ($K_1 = 4.1\ dm^3 mol^{-1}$, with HCl), which generates the ethyl species. At low concentrations of acid subsequent rate-limiting intramolecular migration of a hydrogen atom from the remote carbon atom of the ethyl ligand to the metal (β-hydrogen transfer) forms the hydrido product ($k_3 = 0.15\ s^{-1}$). At higher concentrations of acid a further pathway involving direct protonation of *trans*-[W(η^2-C_2H_4)$_2$(dppe)$_2$] at the metal contributes to the reaction. This latter pathway is associated with a significant primary isotope effect ($k_3^H/k_3^D = 2.43$).

Thus, although the stoichiometric equation indicates that the ethene ligands are innocent spectators to the reaction occurring at the metal site, mechanistic studies show that in at least one of the pathways the ethene ligands are intimately involved in transferring the proton to the metal. This noninnocent role for the ethene ligands is confirmed in the studies between *trans*-[W(η^2-C_2H_4)$_2$(dppe)$_2$] and an excess of anhydrous ^{2}HBr. Isolation of the product and its characterization by ^{2}H NMR spectroscopy showed that deuterium was incorporated both at the hydride position and in the ethene ligands.

In *trans*-[W(η^2-C_2H_4)$_2$(dppe)$_2$] the rate of protonation of the coordinated ethene can be estimated as $k_1 \geq 1 \times 10^6\ dm^3 mol^{-1} s^{-1}$, and the rate of protonation of tungsten is $k_2 = 2 \times 10^2\ dm^3 mol^{-1} s^{-1}$. Hence the rate of protonation of the carbon is at least ten thousand times faster than at the tungsten. In the analogous molybdenum system, the ethene is again protonated more rapidly than the metal but now by only a factor of 100. This less marked difference in the molybdenum complex is because the protonation at molybdenum is faster than at tungsten in analogous complexes. Studies on the proton transfer reactions of metal hydride complexes indicate that the rate constant for metal-to-metal proton transfer decreases down a group: Cr > Mo $\gg$ W.

These studies on *trans*-[M(η^2-C_2H_4)$_2$(dppe)$_2$] (M = Mo or W) define unambiguously the more rapidly protonated site. However, this is the exception rather than the rule. For instance, in the closely related propyne complex *trans*-[Mo(η^2-MeCCH)$_2$(dppe)$_2$], the propyne gives the vinyl species *trans*-[Mo(CHCHMe)(η^2-MeCCH)(dppe)$_2$]$^+$ within 2 ms. However, the proton's route to this site cannot be identified. It is possible that the proton adds either directly to the carbon site or binds initially to the metal with subsequent intramolecular migration to the carbon. In the latter case a lower limit for the rate of protonation of the metal can be estimated as $k \geq 1 \times 10^6\ dm^3 mol^{-1} s^{-1}$. This value is much faster than the rate constant for protonation of the metal site in the analogous ethene complex, but is still ten thousand times slower than the diffusion-controlled limit.

The chemistry established in this system is the foundation of the work on product specificity discussed in Section 4.

4. Using Protons as a Means of Product Control

In the discussion so far three general mechanistic principles have emerged for the protonation of complexes containing unsaturated hydrocarbons: 1) The initial site of protonation may not be the final residence of the proton. 2) Protonation can occur at both the metal and the hydrocarbon ligands. 3) Acid-catalyzed or intramolecular rearrangements can, in effect, transfer a proton between the metal and the ligand.

In the remainder of this article we shall see how these mechanistic features, and in particular that protonation can occur either the carbon or the metal, can be used to our advantage—first to control the selective production of alkane, alkene, or alkyne from alkene-based complexes, and second to control the stereochemistry of hydrocarbon products.

4.1. Protonation of *trans*-[Mo(η^2-C_2H_4)$_2$(dppe)$_2$]: Formation of Ethene and Ethane

The protonation of *trans*-[Mo(η^2-C_2H_4)$_2$(dppe)$_2$] with anhydrous HCl gives mixtures of ethane and ethene together with well-defined metal complexes. A limiting stoichiometric reaction is given by Equation (18); however, as we shall see later,

$$trans\text{-}[Mo(\eta^2\text{-}C_2H_4)_2(dppe)_2] + 2HCl \longrightarrow trans\text{-}[MoCl_2(dppe)_2] + C_2H_4 + C_2H_6 \quad (18)$$

this equation is only valid at relatively low concentrations of acid; at high concentrations of acid other products are formed.[35] Clearly this is a multistage reaction involving, at the very least, diprotonation of one of the ethene ligands, transfer of two electrons from the metal to the protonated ligand, release of one molecule each of ethene and ethane, and the binding of two chlorine atoms to the molybdenum center. This complexity is reflected in the stopped-flow absorbance–time trace for this reaction (Fig. 3). Three distinct stages are evident: an initial absorbance jump, complete within the dead time of the apparatus, is followed by an exponential absorbance decrease and finally an absorbance increase, which is also exponential. This trace is a kineticist's dream that can rapidly become a nightmare in trying to define what elementary reactions are associated with each stage. If we were to come "cold" to this multistage trace, there would be little chance of unambiguously identifying the steps occurring at each stage. However, the previous study on the analgous tungsten complex described in Section 3.5 has identified the characteristic behavior associated with the initial protonation of this type of complex.

The first two stages of the reaction of HCl with *trans*-[Mo(η^2-C_2H_4)$_2$(dppe)$_2$] recorded with a stopped-flow apparatus show behavior similar to that observed for the tungsten analogue (Section 3.5): an initial absorbance decrease, complete within

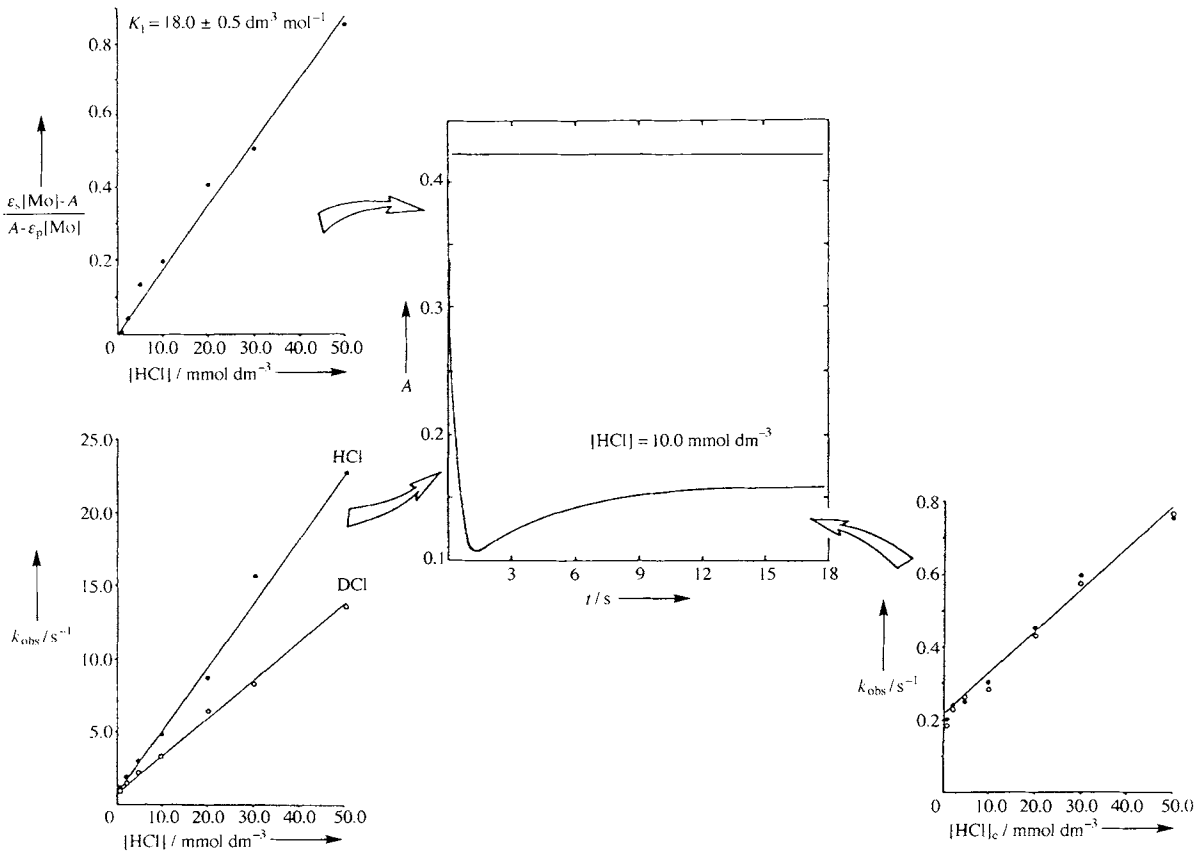

Fig. 3. The protonation of *trans*-[Mo(η^2-C_2H_4)$_2$(dppe)$_2$] to form ethene and ethane: the experimental absorbance–time trace and the dependence of the rates of relevant stages of the reaction on acid concentration ([Mo]: total molybdenum concentration, ε_s: extinction coefficient of the starting material, ε_p: extinction coefficient of the product [HCl]$_c$ = [HCl] − [Mo] (corrected acid concentration)).

2 ms, whose magnitude depends on the concentration of acid, followed by an exponential decay; the latter process shows a dependence on the concentration of HCl as illustrated in Figure 3.[34] Consequently, we can be confident that these first two phases correspond to the formation of the hydrido species [MoH(η^2-C_2H_4)$_2$(dppe)$_2$]$^+$ by two pathways: 1) rapid protonation of the ethene ligand ($K_1 = 18$ dm^{3}mol^{-1}), followed by intramolecular β-hydrogen transfer from the ethyl ligand to the metal ($k_3 + k_{-3}$) = 0.22 s^{-1}, and 2) direct protonation of the metal in *trans*-[Mo(η^2-C_2H_4)$_2$(dppe)$_2$] ($k_2 = 4.6 \times 10^2$ dm^{3}mol^{-1}s^{-1}, $k_H/k_D = 1.64$, Scheme 11). The only difference between this system and the protonation of the tungsten complex is that in this molybdenum system an equilibrium mixture of the parent complex, the ethyl complex, and the hydrido species is produced. This conclusion is consistent with previous work,[36] which showed that in solution [Mo(C_2H_5)(η^2-C_2H_4)(dppe)$_2$]$^+$ is in dynamic equilibrium with [MoH(η^2-C_2H_4)$_2$(dppe)$_2$]$^+$ and that the magnitude of the absorbance changes for these stages depend upon the acid concentration.

A further absorbance increase is observed over the last 20 seconds of the absorbance–time trace, the magnitude and rate of which depends on the concentration of acid. This stage corresponds to the protonation of the equilibrium mixture of *trans*-[Mo(η^2-C_2H_4)$_2$(dppe)$_2$], [MoH(η^2-C_2H_4)$_2$(dppe)$_2$]$^+$, and [Mo(C_2H_5)(η^2-C_2H_4)(dppe)$_2$]$^+$ to produce the dihydrido species [MoH$_2$(η^2-C_2H_4)$_2$(dppe)$_2$]$^{2+}$.

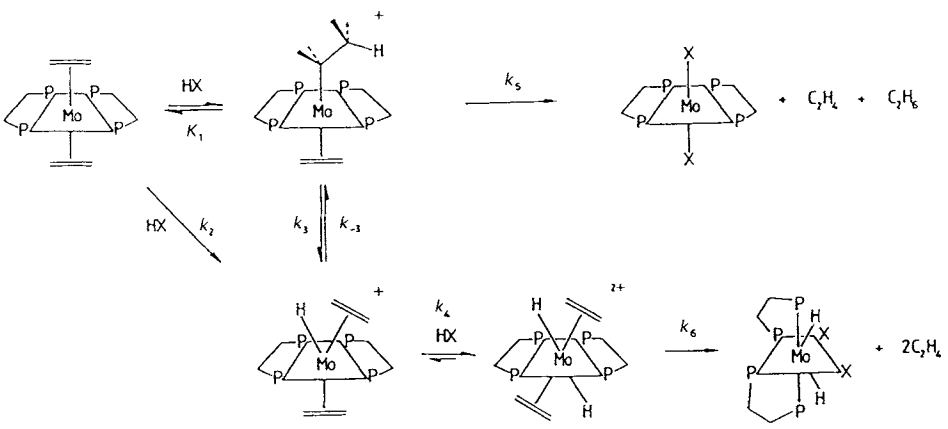

Scheme 11. Elementary reactions for the protonation of *trans*-[Mo(η^2-C_2H_4)$_2$(dppe)$_2$] to form ethene and ethane.

The kinetics of the third stage exhibits a simple two-term rate law: one term is independent of the concentration of acid and the other shows a first-order dependence on the concentration of acid. Protonation of the equilibrium mixture formed at the end of the second stage disturbs the position of this

equilibrium, and analysis of the kinetics for the third stage reveals that the term independent of the concentration of acid corresponds to $(k_3 + k_{-3})$, that is, to the sum of the rate constants for the equilibrium between $[Mo(C_2H_5)(\eta^2\text{-}C_2H_4)(dppe)_2]^+$ and $[MoH(\eta^2\text{-}C_2H_4)_2(dppe)_2]^+$. The value of $(k_3 + k_{-3})$ is already known from the analysis of the kinetics of the second stage and is in excellent agreement with the value derived from analysis of the third stage.

The discussion so far presents an internally consistent kinetic model for the early stages of the reaction of *trans*-$[Mo(\eta^2\text{-}C_2H_4)_2(dppe)_2]$, and this mechanistic behavior is reconcilable with that of the tungsten analogue. However, the identity of the intermediates has been confirmed by spectroscopic detection, isolation, and characterization. In particular the species formed at the end of the second stage has the same electronic spectrum as that of isolated $[MoH(\eta^2\text{-}C_2H_4)_2(dppe)_2]HCl_2$. However, as is typical of electronic spectra in general, this spectrum consists of rather broad peaks and is not particularly diagnostic. Certainly no structural information about the intermediate can be obtained by this method. A much better identification of the intermediates results from studying the reactions in the probe of an NMR spectrometer.

Figure 4 illustrates the course of reaction (18) as monitored by $^{31}P\{^1H\}$ NMR spectroscopy. In order to detect the intermediates, which at room temperature only have a fleeting existence, the reaction is performed at relatively low concentrations of acid and low temperatures (typically $-80\,^\circ C$). The use of $^{31}P\{^1H\}$ NMR spectroscopy has the advantage that only signals associated with the complex are present, and the other components of the mixture (the acid and solvent etc.) do not complicate the spectrum. The singlet at $\delta = -78$ in the first spectrum of this series is that of the parent complex, *trans*-$[Mo(\eta^2\text{-}C_2H_4)_2(dppe)_2]$. As time passes, this peak decreases in intensity, and a new set of signals appear [$\delta = -80.0$ (d), $\delta = -92.2$ (d); $J_{P,P} = 81.8$ Hz; AA'BB' pattern]. The intensity of this pair of doublets increases, then slowly decreases as, finally, the peaks of one of the products appear. The spectrum that consists of a deceptively simple pair of doublets is that of the equilibrium mixture of $[Mo(C_2H_5)(\eta^2\text{-}C_2H_4)(dppe)_2]^+$ and $[MoH(\eta^2\text{-}C_2H_4)_2(dppe)_2]^+$ and has been observed in earlier variable temperature studies on this[36] and analogous systems.[37] However, this is the first time this spectrum has been observed for an intermediate in the protonation reactions of *trans*-$[Mo(\eta^2\text{-}C_2H_4)_2(dppe)_2]$.

This study confirms the nature of the intermediates at the end of the second stage, which was proposed on the basis of the kinetic analysis. Furthermore, at higher concentrations of acid we observe the expected contribution to the spectrum associated with the presence of $[MoH_2(\eta^2\text{-}C_2H_4)_2(dppe)_2]^{2+}$. The spectrosopic changes are similar to those shown in Figure 4, but now the spectrum of the intermediate is slightly different. It still consists of a pair of doublets, but the chemical shift separation between the doublets is smaller [$\delta = -76.2$ (d), $\delta = -92.2$ (d)], and the doublet separation itself (which is the phosphorus–phosphorus coupling constant, $J_{P,P} = 73.5$ Hz) is about 8 Hz smaller than in the spectrum observed at low concentrations of acid. The spectrum at high acid concentrations is consistent with the presence of a species that is structurally similar to that detected at low concentrations of acid, and the smaller value of $J_{P,P}$ indicates an increased protonation of the metal.[38]

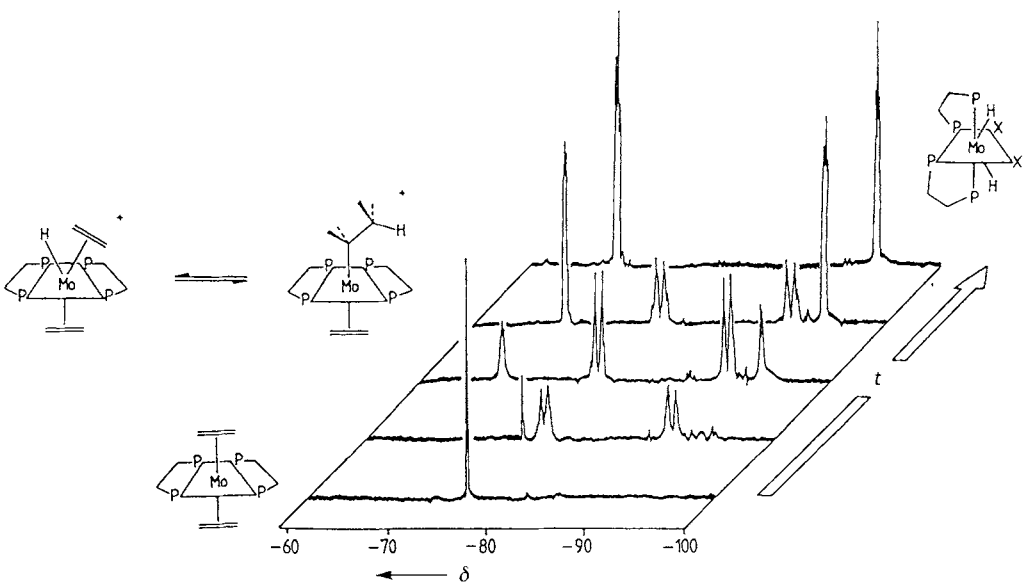

Fig. 4. The time course of the protonation of *trans*-$[Mo(\eta^2\text{-}C_2H_4)_2(dppe)_2]$ to form ethene and ethane, monitored by $^{31}P\{^1H\}$ NMR spectroscopy.

$[MoH(\eta^2\text{-}C_2H_4)_2(dppe)_2]HCl_2$ has been isolated from the reaction mixture at low concentrations of acid by rapid crystallization, but attempts to isolate $[MoH_2(\eta^2\text{-}C_2H_4)_2(dppe)_2]^{2+}$ were unsuccessful, even at high concentrations of acid. The only species isolated was the monohydride, presumably because of the poorer solubility of this species and the rapidity of the monohydride–dihydride protonation equilibrium.

The multiple protonation equilibria shown in Scheme 11 are established within about 20 s. However, the evolution of both ethane and ethene (monitored by GLC) from the reaction mixture has a half-life of about 40 min. The rate of formation of either hydrocarbon is independent of the concentration of acid, but the relative proportions of ethane and ethene depend markedly on the concentration of acid (Fig. 5). Thus at relatively low concentrations of HCl one equivalent each of ethane and ethene are produced. At higher concentrations of acid the carbon mass-balance is maintained, but the proportion of ethane progressively decreases, and the proportion of ethene increases correspondingly until, at $[HCl] \approx 200$ mmol dm^{-3}, two equivalents of ethene are produced.

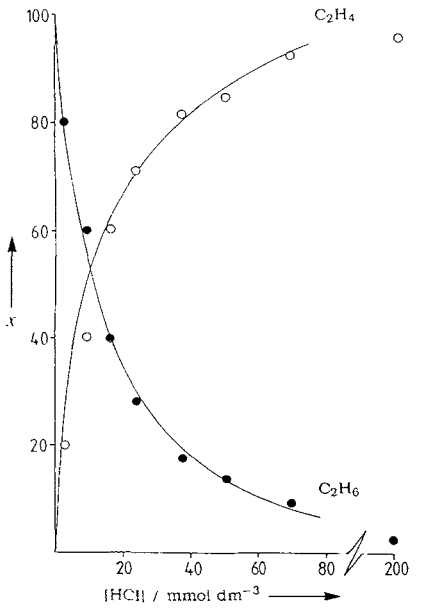

Fig. 5. Dependence of the product distribution on the acid concentration for the protonation of *trans*-[Mo(η^2-C_2H_4)$_2$(dppe)$_2$].

The mechanism by which these hydrocarbons are formed is shown in Scheme 11. At low concentrations of HCl the predominant species in solution are the complexes of the equilibrium mixture of *trans*-[Mo(η^2-C_2H_4)$_2$(dppe)$_2$], [MoH(η^2-C_2H_4)$_2$-(dppe)$_2$]$^+$, and [Mo(C_2H_5)(η^2-C_2H_4)(dppe)$_2$]$^+$. Rate-limiting dissociation of the ethene ligand from [Mo(C_2H_5)(η^2-C_2H_4)(dppe)$_2$]$^+$, followed by rapid attack of chloride at the metal commits the ethyl ligand to form ethane, presumably by rapid protonation of the ethyl ligand. Thus, under these conditions, one equivalent each of ethene and ethane are produced together with *trans*-[MoCl$_2$(dppe)$_2$].

At higher concentrations of HCl further protonation occurs at the metal, and [MoH$_2$(η^2-C_2H_4)$_2$(dppe)$_2$]$^{2+}$ dominates the equilibrium mixture. This further protonation at the metal labilizes both ethene ligands towards dissociation, and thus at high concentrations of acid two equivalents of ethene are produced together with [MoH$_2$Cl$_2$(dppe)$_2$].

The product [MoH$_2$Cl$_2$(dppe)$_2$] has been isolated and characterized. Indeed it is this species whose spectrum is observed in the last spectrum recorded in Figure 4. The product formed at low concentrations of acid, *trans*-[MoCl$_2$(dppe)$_2$], has also been isolated and characterized by the common techniques, in particular by its characteristic electrochemical behavior.[39] However, this compound has a d^4 ($S = 1$) configuration and is silent in both EPR and NMR spectroscopy.

The mechanism shown in Figure 3 quantitatively predicts the hydrocarbon product distribution. Since the rate of production of both ethane and ethene is essentially the same, the composition of the hydrocarbon mixture varies with the concentration of HCl according to Equation (19), which has made allowance

$$\frac{[C_2H_6]}{[C_2H_6]+[C_2H_4]} = \frac{k_3 + k_{-3}}{(k_3 + k_{-3}) + k_4[HCl]} \quad (19)$$

for the fact that one equivalent of ethene is produced in both pathways. All the elementary rate constants in this equation are known from the kinetic analysis. When the values are substituted into this equation the curves obtained are an excellent fit to the experimental product distribution as shown in Figure 5.

One of the most important aspects of this hydrocarbon product distribution is that it is counterintuitive. After all, in order to produce ethane by the protonation of an ethene ligand, the ethene must be supplied with two electrons and two protons. In a system such as that described here, where the two electrons are already "stored" in the metal, it would seem intuitive that the higher the concentration of acid, the more likely it is that the ethene will protonate, and hence it would be predicted that ethane would be produced preferentially at high concentrations of acid. This is the opposite to the behavior actually observed. However, the observed product distribution is readily understood when it is appreciated that protonation can occur at either the metal or the hydrocarbon, and the site that is protonated defines the hydrocarbon product.

The mechanism in Scheme 11 shows that there is no problem in protonating the ethene in these complexes (indeed it is these ligands which are protonated most rapidly), and when protonated ethane is produced. However, at high concentrations of acid further protonation of the metal occurs and results in the deactivation of the ethene ligand towards protonation and the labilization of the system to the dissociation of ethene.

Just by adding protons the product of the reaction can be controlled. The origin of this control is the sites of protonation: metal or ligand. The product of the reaction can also be controlled after the protonation step by changing the coligands on the complex as illustrated in Scheme 12. Having formed *trans*-

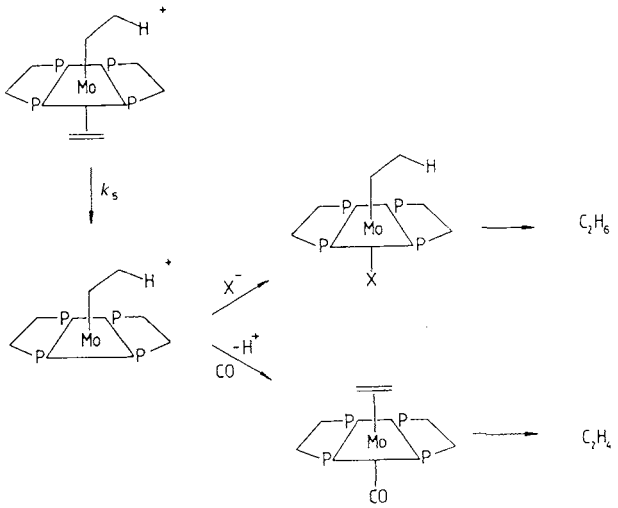

Scheme 12. Controlling the product distribution after the protonation of [Mo(C_2H_5)(η^2-C_2H_4)(dppe)$_2$]$^+$ by varying the coligands.

[Mo(C_2H_5)(η^2-C_2H_4)(dppe)$_2$]$^+$, rate-limiting dissociation of the ethene ligand is usually followed by binding of chloride. However, carbon monoxide can bind preferentially to form *trans*-[Mo(C_2H_5)(CO)(dppe)$_2$]$^+$. The electron-withdrawing effect of the coordinated carbon monoxide results in proton loss from the ethyl ligand, subsequent release of ethene, and ultimate formation of *trans*-[Mo(CO)$_2$(dppe)$_2$]. Thus, even at low concentrations of acid the system can be forced to evolve only ethene if the coordination sphere of the complex is perturbed.

Under an atmosphere of dihydrogen the situation is less clear cut, but about 20% of the hydrocarbon released at an HCl concentration of 200 mmol dm^{-3} is ethane, whereas under an atmosphere of argon no ethane is produced under these condi-

tions. It would therefore appear that dihydrogen can also bind to the vacant site generated on dissociation of ethene from $[MoH_2(\eta^2\text{-}C_2H_4)_2(dppe)_2]^{2+}$ to form a species (presumably $[MoH_4(\eta^2\text{-}C_2H_4)(dppe)_2]^{2+}$), which is sufficiently hydride-rich to produce some ethane from this route.

4.2. Protonation of *trans*-$[MoH(\eta^3\text{-}C_3H_5)(dppe)_2]$: Formation of Propene and Propyne

The protonation of any alkene other than ethene introduces another potential type of reactivity, which is a consequence of the intramolecular rearrangement possible with higher alkenes shown in Scheme 13. Only one molecule of propene will bind to

Scheme 13. The dynamic equilibrium between $[Mo(\eta^2\text{-}MeCHCH_2)(dppe)_2]$ and $[MoH(\eta^3\text{-}C_3H_5)(dppe)_2]$ illustrating the additional pathway for higher alkenes.

the $\{Mo(dppe)_2\}$ site, and variable temperature NMR spectroscopy has shown that $[Mo(\eta^2\text{-}MeCHCH_2)(dppe)_2]$ is in dynamic equilibrium with $[MoH(\eta^3\text{-}C_3H_5)(dppe)_2]$.[36] The solid state structure of this complex and the tungsten analogue has been established by X-ray crystallography.[40] The structures are essentially the same, and that of $[WH(\eta^3\text{-}C_3H_5)(dppe)_2]$ is shown in Figure 6. Two important structural features evident

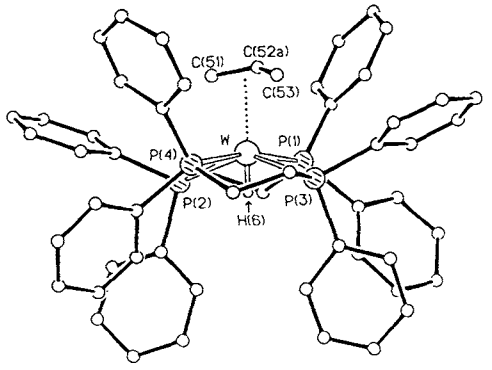

Fig. 6. The crystal structure of $[MoH(\eta^3\text{-}C_3H_5)(dppe)_2]$. Selected bond lengths [Å] and the angle of the allyl group [°]: W-P(average) 2.465 ± 0.007, W-C51 2.372(16), W-C53 2.334(14), W-C52a 2.258(30), C51-C52a 1.35(4), C53-C52a 1.23(4), W-H 1.03(9); C51-C52a-C53 139(3).

from this study are pertinent to the discussion of the reactivity of this complex. First, the hydride (which was located) is *trans* to the allyl group; but, clearly, in solution this hydride must move around the metal surface if it is to transfer intramolecularly to the allyl residue. Second, there is nothing unusual about the geometry of the allyl group: the carbon–carbon bond lengths are typical of an allyl group and the CCC angle is not flattened. The reactivity that $[MoH(\eta^3\text{-}C_3H_5)(dppe)_2]$ exhibits in its reactions with anhydrous HCl [Eqs. (20) and (21)] led us to look for

$$trans\text{-}[MoH(\eta^3\text{-}C_3H_5)(dppe)_2] + 2HCl \longrightarrow [MoH_2Cl_2(dppe)_2] + MeCHCH_2 \quad (20)$$

$$trans\text{-}[MoH(\eta^3\text{-}C_3H_5)(dppe)_2] + 2HCl \longrightarrow [MoH_2Cl_2(dppe)_2] + H_2 + MeCCH \quad (21)$$

such a distortion in this molecule.[41] At all acid concentrations the same metal product, $[MoH_2Cl_2(dppe)_2]$ is formed. However, the hydrocarbon product is propene at low concentrations of HCl, but propyne at high concentrations of acid. That is, by protonating a complex derived from an alkene we can produce an alkyne!

In order to understand this reaction in more detail it has been studied mechanistically. Before the mechanism is discussed a further structural aspect of the work has to be clarified. The equilibrium between the propene and allyl forms of the molybdenum complex is rapid at 25.0 °C, and thus it is unclear which form is the reactive entity in the protonation reactions. Two-dimensional $\{^1H\text{-}^{13}C\}$ NMR spectroscopy has been used to assign unambiguously the peaks in the ^1H NMR spectrum that are attributable to $[Mo(\eta^2\text{-}MeCHCH_2)(dppe)_2]$ and $[MoH(\eta^3\text{-}C_3H_5)(dppe)_2]$. In this way it was established that at −40 °C the allyl species only is present. At this temperature, the system still reacts with HCl to form propyne at high concentrations of acid. This indicates that the allyl form is the reactive species, and this is confirmed in studies with the tungsten analogue.[42] *trans*-$[WH(\eta^3\text{-}C_3H_5)(dppe)_2]$ is always in the allyl form; even at +40 °C there is no sign of the propene species, and the hydride signal ($\delta = -2.8$, quintet, $J_{H,P} = 35$ Hz) is still well resolved. This complex reacts with anhydrous acid to produce propene at low concentrations of acid and propyne at high concentrations of acid.

A study of the reaction of *trans*-$[MoH(\eta^3\text{-}C_3H_5)(dppe)_2]$ with an excess of anhydrous HCl on a stopped-flow apparatus shows the same simple behavior under all conditions: an exponential absorbance–time decay.[41] The final absorbance apparently corresponds to that of the product, $[MoH_2Cl_2(dppe)_2]$ (see later discussion), but the initial absorbance is slightly lower than that expected for *trans*-$[MoH(\eta^3\text{-}C_3H_5)(dppe)_2]$. The difference between the expected and the observed initial absorbance is independent of the concentration of acid. The reaction exhibits a first-order dependence on the concentration of complex and a dependence on the concentration of HCl as described by Equation (22). These simple kinetics are to be contrasted with the

$$k_{obs} = k_3 + k_4[HCl] \quad (22)$$

hydrocarbon product distribution shown in Figure 7, which changes quite dramatically in the acid concentration range over which the kinetics are defined. At low concentrations of acid, propene is the predominant product. At higher concentrations of acid, the carbon mass-balance is maintained, but the proportion of propene decreases whilst the amount of propyne increases proportionately until at $[HCl] > 200$ mmol dm^{-3} propyne is the exclusive product. This behavior is analogous to that observed with the ethene system: the more unsaturated hydrocar-

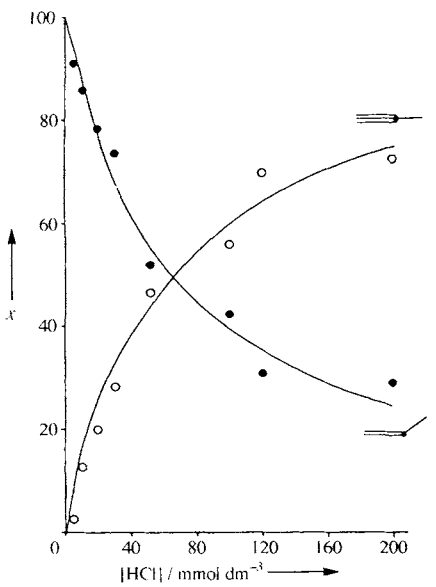

Fig. 7. The dependence of the hydrocarbon product distribution on acid concentration for the protonation of *trans*-[MoH(η^3-C_3H_5)(dppe)$_2$].

bon is formed only at the higher concentrations of acid. The mechanism of the reaction is shown in the lower portion of Scheme 14. Initial, rapid protonation of *trans*-[MoH(η^3-C_3H_5)(dppe)$_2$] at either the metal or the allyl group produces [MoH_2(η^3-C_3H_5)(dppe)$_2$]$^+$ and [MoH(η^2-MeCHCH$_2$)(dppe)$_2$]$^+$, respectively. The cationic propene complex subsequently undergoes rate-limiting dissociation of the propene ($k_3 = 4.3\,s^{-1}$) and ultimate formation of [MoH_2Cl_2(dppe)$_2$].

At low concentrations of acid, any [MoH_2(η^3-C_3H_5)(dppe)$_2$]$^+$ formed converts into [MoH(η^2-MeCHCH$_2$)(dppe)$_2$]$^+$, either by an intramolecular migration, or by proton dissociation to reform the parent allyl complex. Hence, under these conditions, one equivalent of propene is formed.

At higher concentrations of acid a further protonation of [MoH_2(η^3-C_3H_5)(dppe)$_2$]$^+$ can occur, probably at the allyl group to form [MoH_2(η^2-MeCHCH$_2$)(dppe)$_2$]$^{2+}$ (k_4 = 3.8×10^3 dm^3 mol^{-1} s^{-1}), and this commits the system to the formation of propyne. The important mechanistic point is that this second protonation labilizes the system, not to the loss of hydrocarbon but to the preferential loss of dihydrogen. It seems most likely that the dissociation of dihydrogen generates a coordinatively unsaturated, formally fourteen-electron species, [Mo(η^2-MeCHCH$_2$)(dppe)$_2$]$^{2+}$. In order to counteract this electron deficiency the metal dehydrogenates the coordinated propene to generate the formally sixteen-electron propyne species, [MoH_2(η^2-MeCCH)(dppe)$_2$]$^{2+}$, from which propyne subsequently dissociates. At high concentrations of acid, protonation of [MoH_2(η^3-C_3H_5)(dppe)$_2$]$^+$ is faster than dissociation of propene from [MoH(η^2-MeCHCH$_2$)(dppe)$_2$]$^+$, so under these conditions this propene complex converts into [MoH_2(η^3-C_3H_5)(dppe)$_2$]$^+$ and one equivalent of propyne is formed.

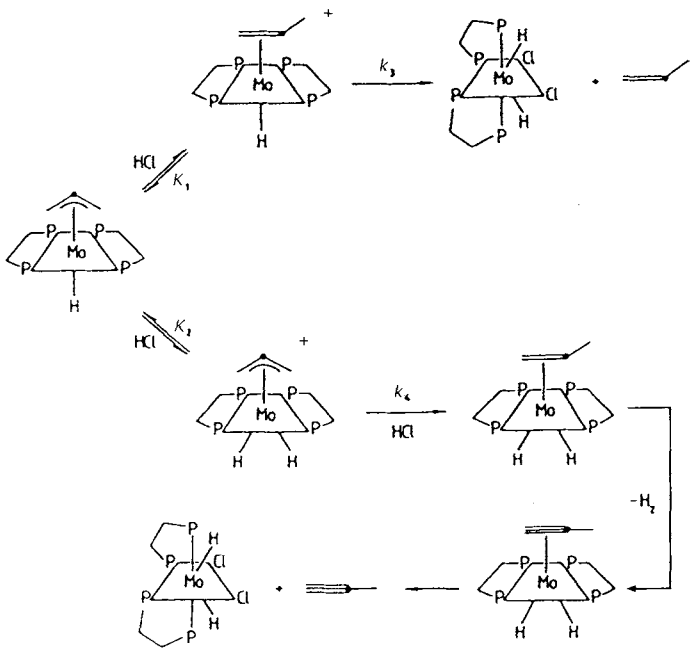

Scheme 14. Proposed mechanism for the formation of propene and propyne by the protonation of *trans*-[MoH(η^3-C_3H_5)(dppe)$_2$].

The hydrocarbon product distribution that this mechanism predicts is given by Equation (23). The elementary rate and

$$\frac{[\text{MeCCH}]}{[\text{MeCCH}] + [\text{MeCHCH}_2]} = \frac{k_4[\text{HCl}]}{k_4[\text{HCl}] + k_3(K_1/K_2)} \qquad (23)$$

equilibrium constants in this equation are known from the kinetic analysis, except for the ratio K_1/K_2. However, the best fit to the data is obtained when $K_1/K_2 \approx 50$. This is similar behavior to that observed with *trans*-[Mo(η^2-C_2H_4)$_2$(dppe)$_2$]: protonation of the hydrocarbon ligand is more favorable than protonation of the metal.

The details of how the propene and propyne are formed from [MoH(η^2-MeCHCH$_2$)(dppe)$_2$]$^+$ and [MoH_2(η^2-MeCHCH$_2$)(dppe)$_2$]$^{2+}$, respectively, are still not fully understood, and clearly more detail concerning these steps is required. The time course for the production of propene and propyne is shown in Figure 8a.[42] Propene is evolved quantitatively within about two minutes whereas it takes about an hour to produce the propyne quantatively. This indicates that the final absorbance observed in the stopped-flow experiments at high concentrations of acid is not that of [MoH_2Cl_2(dppe)$_2$], but rather corresponds to a precursor whose electronic spectrum is similar to that of the dichloro product. It seems likely that this precursor is [MoH_2(η^2-MeCCH)(dppe)$_2$]$^{2+}$, which slowly evolves propyne. In addition it is clear that dihydrogen evolution precedes propyne evolution consistent with the proposed mechanism.

Intermediates in the propyne-forming pathway have been detected by low temperature $^{31}P\{^1H\}$ NMR spectroscopy (Fig. 8b).[42] The spectra recorded for relatively low concentrations of acid are shown on the right. In the first spectrum the peak in the correct position for *trans*-[MoH(η^3-C_3H_5)(dppe)$_2$] is significantly broadened. This broadening is due in part to the low temperature, but mostly because the spectrum corresponds to the equilibrium mixture of *trans*-[MoH(η^3-C_3H_5)(dppe)$_2$], *trans*-[MoH(η^2-MeCHCH$_2$)(dppe)$_2$]$^+$, and *trans*-[MoH_2(η^3-C_3H_5)(dppe)$_2$]$^+$. As time passes this broad peak slowly decreases in intensity, and the only new peaks that appear are those of the product, [MoH_2Cl_2(dppe)$_2$]. No intermediates are detected under these conditions indicating that only short-lived species are generated on the propene-forming pathway.

At high concentrations of acid the propyne-forming pathway will dominate, and under these conditions at least three intermediates are detectable, as shown on the left of Figure 8b. As the broad peak associated with the protonation equilibria species

decreases in intensity three new sets of signals appear consecutively: the first around the initial peak, the second at high field, and the third at intermediate field. Finally, the peaks attributable to the product $[MoH_2Cl_2(dppe)_2]$ appear. To date we have not been able to identify these intermediates unambiguously, or isolate them, even at low temperatures. However, a noticeable feature of these spectra is the pairs of doublets in the last two sets of signals. This is reminiscent of the spectrum of the intermediates observed in the reaction of *trans*-$[Mo(\eta^2\text{-}C_2H_4)_2(dppe)_2]$, and it is tempting to assign these signals to the species $[MoH_2(\eta^2\text{-}MeCHCH_2)(dppe)_2]^{2+}$ and $[MoH_2(\eta^2\text{-}MeCCH)(dppe)_2]^{2+}$.

We do not understand the factors which discriminate between the evolution of dihydrogen and the evolution of a hydrocarbon upon protonation of a complex. This is a crucial aspect of the reactivity in the $[MoH(\eta^3\text{-}C_3H_5)(dppe)_2]$. Recent studies on the reaction of $[MoH_3(CCt\text{Bu})(dppe)_2]$ with anhydrous HCl shown in Equation (24) demonstrate that the rate of coupling of two-hydrogen atoms and the rate of coupling a hydrogen atom with the alkynyl differ by less than a factor of 20.

$$[MoH_3(CCt\text{Bu})(dppe)_2] + 2HCl \longrightarrow [MoH_2Cl_2(dppe)_2] + t\text{BuCCH} + H_2 \quad (24)$$

4.3. Protonation of $[MoH(\eta^3\text{-}C_4H_7)(dppe)_2]$: Dimerization of an Alkene

One of the major problems in defining the details of the formation of either propene or propyne from *trans*-$[MoH(\eta^3\text{-}C_3H_5)(dppe)_2]$ is that the two pathways operate simultaneously. It would be advantageous if the formation of one hydrocarbon product could be studied in isolation over a wide acid concentration range. The conversion of the allyl ligand into propyne must involve the removal of the hydrogen atom bound to the central carbon atom. Consequently, protonation of a complex containing a 2-alkylallyl ligand must result only in the formation of the corresponding alkene. With this in mind we attempted to prepare and study the 2-methylallyl analogue of *trans*-$[MoH(\eta^3\text{-}C_3H_5)(dppe)_2]$.

The route used to prepare $[MoH(\eta^3\text{-}C_4H_7)(dppe)_2]$ is analogous to that used for all the compounds discussed in this section, and is shown in Scheme 15.[43] Reduction of $[MoCl_4(dppe)]$ by sodium amalgam, in the presence of dppe and under an atmosphere of isobutene gives, after about 18 hours, the labile, orange complex $[Mo(\eta^2\text{-}Me_2CCH_2)_2(dppe)_2]$. This reduction takes place via a bright green intermediate, which can be isolated and shown to be the molybdenum(II), five-coordinate, sixteen-electron species. This complex contains a 2-methylallyl and a hydrido ligand as confirmed by both ^1H and ^{13}C NMR spectroscopy at room temperature. However, it seems that the 2-methylallyl ligand is sufficiently bulky that two sterically demanding dppe ligands cannot be coordinated through all four phosphorus atoms, and hence one of the dppe ligands is only monodentate. $[MoH(\eta^3\text{-}C_4H_7)(dppe)_2]$ undergoes reversible changes in the NMR spectrum when the temperature is varied. Thus, although at 25.0 °C the species is undoubtedly a 2-methylallyl complex, upon cooling an intramolecular,

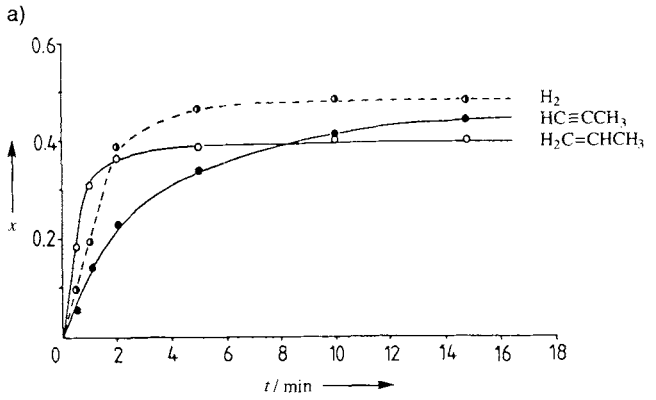

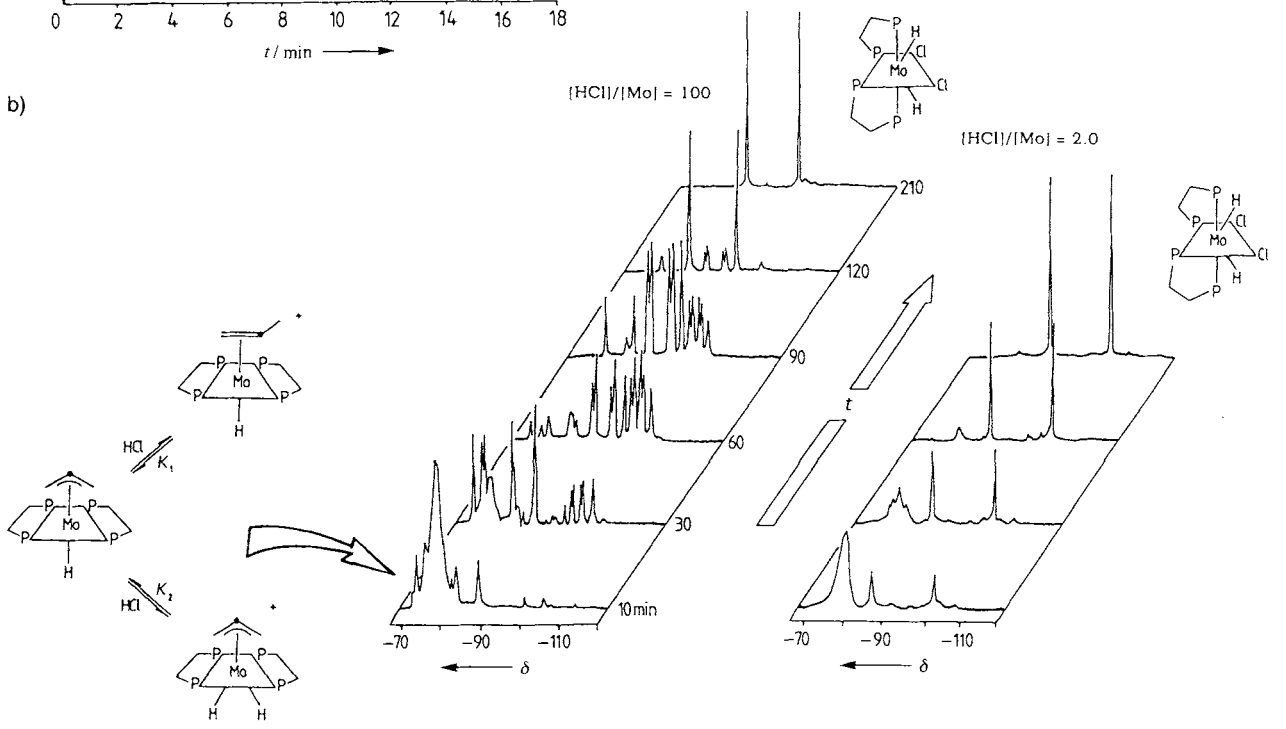

Fig. 8. a) Time course for the evolution of the products in the protonation of *trans*-$[MoH(\eta^3\text{-}C_3H_5)(dppe)_2]$ (x = moles gas per mole complex; b) time course of this reaction monitored by low temperature $^{31}P\{^1H\}$ NMR spectroscopy for [HCl]/[Mo] = 100 (left) and [HCl]/[Mo] = 2 (right).

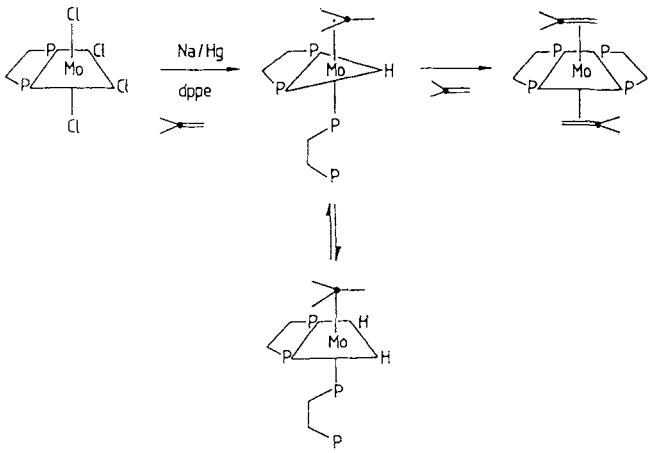

Scheme 15. Synthesis of $[MoH(\eta^3\text{-}C_4H_7)(dppe)_2]$ and its reaction with isobutene to form $[Mo(\eta^2\text{-}Me_2CCH_2)_2(dppe)_2]$.

reversible rearrangement results in the formation of the 18-electron trimethylenemethane dihydrido complex. Parenthetically, it is worth noting that the $\{Mo(dppe)_2\}$ site has been exceptional in demonstrating all the intramolecular rearrangements: alkene/$H^- \rightarrow$alkyl; allyl/$H^- \rightarrow$propene, and trimethylenemethane/$H^- \rightarrow$2-methylallyl.

Protonation of $[MoH(\eta^3\text{-}C_4H_7)(dppe)_2]$ with anhydrous HCl, at room temperature (where it is exclusively in the allyl form) proceeds according to Equation (25). $[MoH_2Cl_2(dppe)_2]$ is a product in all the systems discussed in this section, whilst the hydrocarbon results from the dimerization of isobutene.

$$[MoH(\eta^3\text{-}C_4H_7)(dppe)_2] + 2HCl \longrightarrow [MoH_2Cl_2(dppe)_2] + {}^t BuCH_2C(Me)CH_2 \quad (25)$$

A study of this reaction by the stopped-flow technique shows a single exponential trace with the final absorbance expected for $[MoH_2Cl_2(dppe)_2]$ and an initial absorbance slightly lower than that of the parent complex (Fig. 9). This initial absorbance jump is attributable to the addition of one equivalent of acid, as shown on the left-hand side of Figure 9.

The reaction reflected in the subsequent exponential absorbance–time decay exhibits a first-order dependence on the concentration of complex, but a nonlinear dependence on the concentration of HCl [Fig. 9, right-hand plot; Eq. (26)]. The mechanism of the reaction is shown in Scheme 16. Initial, rapid

$$k_{obs} = \{k_3 + k_4K_2[HCl]\}/(1 + K_2[HCl]) \quad (26)$$

protonation at the metal occurs within 2 ms to form $[MoH_2(\eta^3\text{-}C_4H_7)(dppe)_2]^+$ followed by rate-limiting intramolecular migration of the proton from the metal to the 2-methylallyl ligand ($k_3 = 0.7\ s^{-1}$) produces $[MoH(\eta^2\text{-}Me_2CCH_2)(dppe)_2]^+$. The subsequent steps can not be identified by kinetics, because they occur after the rate-limiting step, but must involve the dimerization of isobutene, and its liberation to form $[MoH_2Cl_2(dppe)_2]$. The complexity of Equation (26) is a consequence of rapid protonation of the pendant phosphorus atom ($K_2 = 52.2\ dm^3 mol^{-1}$). Consequently the kinetics reflect the reactivity of both $[MoH_2(\eta^3\text{-}C_4H_7)(dppe)_2]^+$ and $[MoH_2(\eta^3\text{-}C_4H_7)(dppe)(dppeH)]^{2+}$ ($k_4 = 2.9\ s^{-1}$). This mechanism (in particular the rate-limiting migration steps) is able to rationalize the following kinetic observations: 1) Rate constants associated with apparently acid-

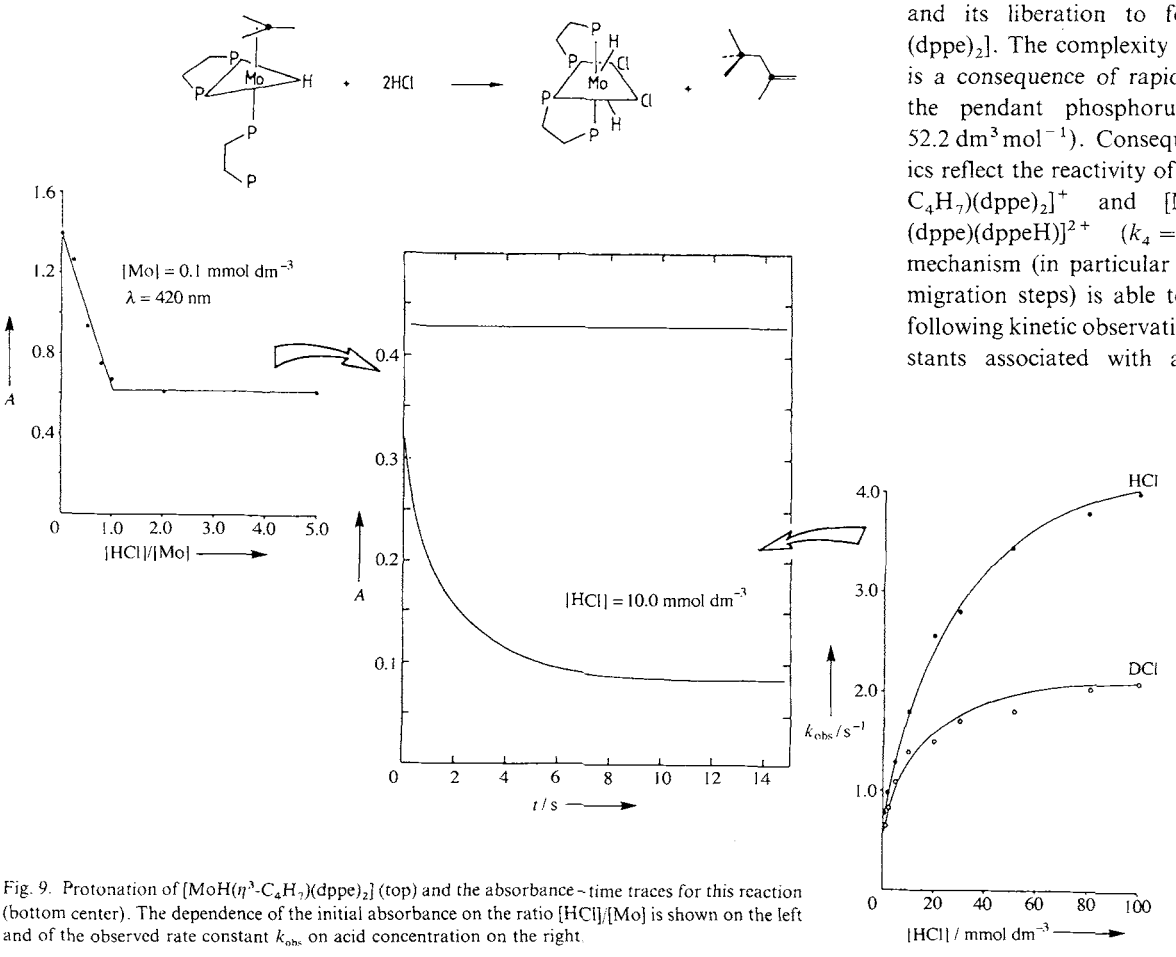

Fig. 9. Protonation of $[MoH(\eta^3\text{-}C_4H_7)(dppe)_2]$ (top) and the absorbance–time traces for this reaction (bottom center). The dependence of the initial absorbance on the ratio [HCl]/[Mo] is shown on the left and of the observed rate constant k_{obs} on acid concentration on the right.

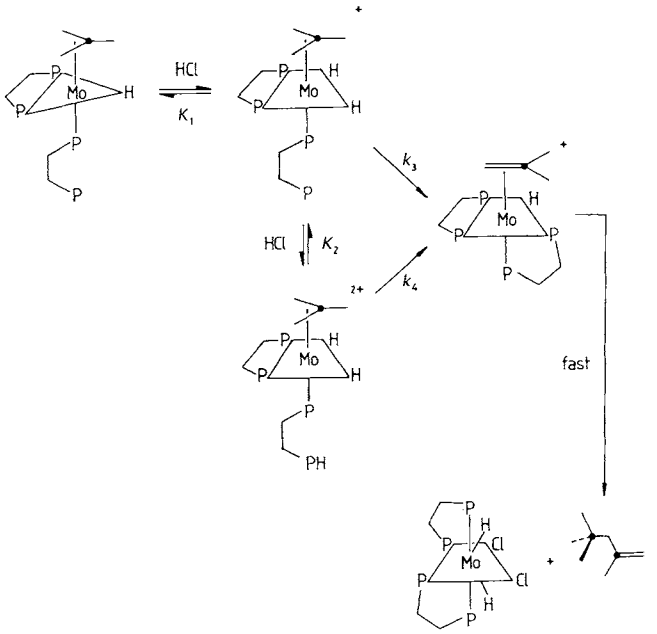

Scheme 16. Proposed mechanism for the protonation of $[MoH(\eta^3\text{-}C_4H_7)(dppe)_2]$ leading to the dimerization of isobutene.

independent steps (k_3 and k_4) exhibit primary isotope effects ($k_3^H/k_3^D = 1.27$, $k_4^H/k_4^D = 1.50$), since these elementary reactions are due to migration of hydrido groups derived from the acid. 2) The initial, rapid reaction consumes one equivalent of acid. 3) As expected, the pendant phosphorus atom is protonated by HCl. An important aspect of the mechanism is that this step is reversible, and thus, towards the end of the reaction, the phosphorus can bind to the metal whilst deprotonated.

The details of the dimerization process are not clear, but it is certainly much faster than the acid-catalyzed dimerization of free isobutene. This indicates that dimerization occurs on the metal site.

4.4. Product Control by Protonation: A Summary

In this section some relatively simple systems have been discussed that when considered together illustrate how the protonation of alkene complexes (or their rearranged analogues) can selectively give alkanes, alkenes, or alkynes as summarized in Scheme 17.

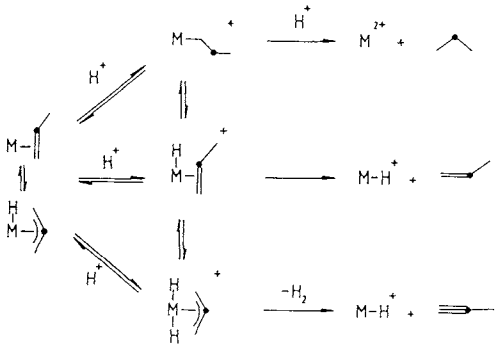

Scheme 17. Protonation of alkene complexes to give alkanes, alkenes, or alkynes, illustrating how selectivity results from protonation at the hydrocarbon or the metal.

The selectivity is a result of protonation at the hydrocarbon or the metal. Thus, protonation at the coordinated alkene gives the alkyl species, which subsequently reacts further to produce an alkane. However, further protonation of the metal occurs at higher concentrations of acid and this labilizes the system towards the release of alkene.

Alkenes higher than ethene can also rearrange on the metal site to form the allyl hydrido species, and this form is capable of producing alkynes upon protonation, if the protonation at the metal preferentially labilizes the release of dihydrogen to generate a coordinatively unsaturated site capable of dehydrogenating the bound alkene.

At first sight it seems anomalous that no propane is formed in the reaction with *trans*-$[MoH(\eta^3\text{-}C_3H_5)(dppe)_2]$. The reason for this is probably kinetic: the formation of propane is slow, and the more rapid formation of either the alkyne or the alkene occur preferentially. It would be interesting to study the products of the reaction between DCl and *trans*-$[MoH(\eta^3\text{-}C_3H_5)(dppe)_2]$ to establish whether any deuterium is incorporated specifically into the secondary carbon of the propene. This would indicate the transient existence of a propyl species that undergoes intramolecular β-hydrogen or deuterium transfer more rapidly than it can form propane.

4.5. Proton-Catalyzed Isomerization of Alkenes

A reaction which has not been observed in the reactions of alkenes bound to the $\{Mo(dppe)_2\}$ site is the acid-catalyzed rearrangements shown in Scheme 18. In principle, protonation

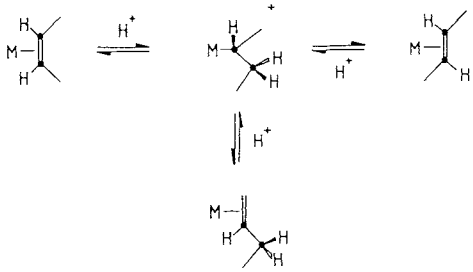

Scheme 18. Acid-catalyzed rearrangements of metal-alkene complexes.

of alkene complexes can give mixtures of *cis*- and *trans*-alkenes together with internal and terminal alkenes via intermediate alkyl species.

Acid-catalyzed *cis*–*trans* isomerization of alkenes bound to rhenium has been observed (Scheme 19).[44] Addition of acid to a solution of the *cis*-2-butene complex $[Re(\eta^5\text{-}C_5H_5)(CO)_2(\eta^2\text{-}cis\text{-}MeCHCHMe)]$ results in the formation of a 45:55 mixture of this *cis*-2-butene complex and $[Re(\eta^5\text{-}C_5H_5)(CO)_2(\eta^2\text{-}trans\text{-}MeCHCHMe)]$ within about 30 min. The proposed mechanism (Scheme 19) involves protonation of the alkene ligand to form the alkyl species, rotation about the carbon–carbon single bond, and deprotonation to generate the equilibrium mixture of alkene complexes.

The exact mechanism by which the alkene is protonated (direct attack at the carbon or via a hydrido species) is unknown, but the most important mechanistic feature is the selectivity that

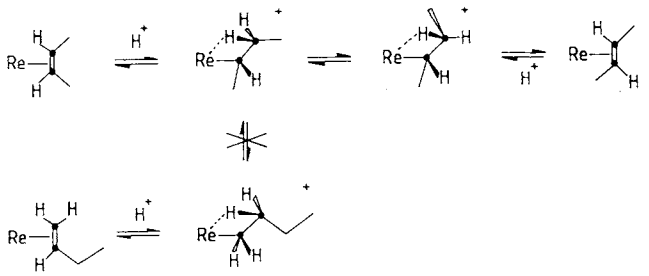

Scheme 19. Isomerization of *cis*-butene on a rhenium center.

shows that both protonation and deprotonation must occur at the same carbon atom: the postulated 2-butyl intermediate does not deprotonate to give the 1-butene complex, and similarly, protonation of the 1-butene complex does not give any 2-butene ligand. This observation can only be rationalized if the two butyl intermediates are different. It has been proposed that the protonation produces an intermediate containing a strong agostic interaction, followed by an "in place rotation" and deprotonation of the agostic alkyl group, which occurs much more rapidly than formation of a free alkyl rhenium intermediate.

A related acid-catalyzed isomerization is the equilibration of coordinated *syn* and *anti* dienes as illustrated for $[Fe(\eta^4\text{-}PhCHCHCHCHBn)(CO)_3]^+$ (Bn = $PhCH_2$) in Scheme 20.[45]

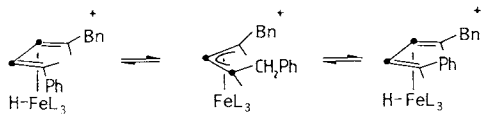

Scheme 20. Equilibration of coordinated *syn* and *anti* dienes at an iron complex. L = CO.

In this example rate-limiting protonation occurs at the metal and is associated with an exceptionally large primary isotope effect ($k_H/k_D = 27$). Intramolecular transfer of the hydrogen from the metal to the diene then forms the allyl species. Subsequent rotation about the carbon–carbon single bond followed by hydrogen migration back to the metal and deprotonation results in equilibration of the *syn* and *anti* isomers.

5. Stereoselective Protonation of Complexes

The addition of protons to coordinated hydrocarbons to produce stereoselective products has been known for some time, especially in the reactions of cyclic polyenes. Thus, as shown in Scheme 21, $[Ni(\eta^5\text{-}C_5H_5)_2]$ is protonated on the cyclopentadienyl ring stereoselectively in the *exo* position.[46] In addition the exchange of ring protons in $[Fe(\eta^5\text{-}C_5H_5)_2]$ involves *exo* attack of a proton at the cyclopentadienyl ring.[47] Subsequently, the *endo* hydrogen transfers to the metal to form $[FeH(\eta^5\text{-}C_5H_5)_2]^+$.

Whether a proton adds directly in *exo* or *endo* position in any particular system cannot be predicted, and examples of both types of addition are known. In many cases there is no clear evidence whether *exo* or *endo* attack has occurred. For instance, the protonation of $[Fe(\eta^4\text{-}C_4H_4)(CO)_3]$ is assumed to involve

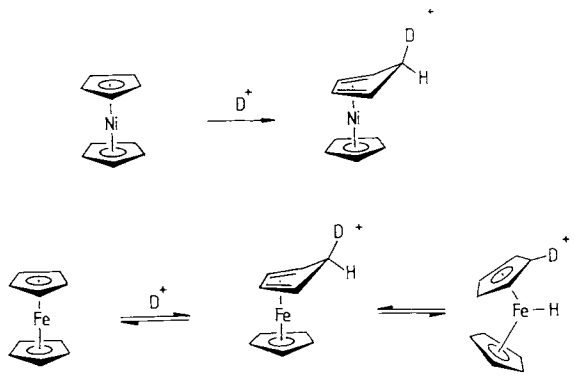

Scheme 21. Stereoselective D^+ attack at the pentadienyl ligand in $[Ni(\eta^5\text{-}C_5H_5)_2]$ and in $[Fe(\eta^5\text{-}C_5H_5)_2]$.

endo attack, since the analogous butadiene complex is protonated in this position.[48] Of course, *endo* addition may involve initial protonation of the metal followed by intramolecular migration. However, the intermediacy of a hydrido species is not essential for formation of *endo* product.

Another aspect of stereoselectivity involves the protonation of alkynes to form *cis*- or *trans*-alkenes selectively. We shall discuss this aspect in detail in this section and show how application of the kinetic principles associated with protonation at the metal or the hydrocarbon ligand outlined so far can be employed to control the stereochemistry of the product.

We saw in the Section 3 that the term regioselective is ambiguous in the sense that although the reaction may amount stoichiometrically to a regioselective protonation, the mechanism whereby this product is formed may not involve direct regioselective attack. A similar problem in terminology occurs for the stereoselectivity of products formed by protonation: the stoichiometrically stereoselective product can be formed by a variety of mechanistic pathways.

5.1. Stereoselectivity in the Protonation of Alkynes: Kinetic Control

Consideration of the protonation of a coordinated alkyne reveals that attack can occur at two faces of the alkyne: *exo* to the metal to give a *trans*-vinyl species or *endo* to the metal giving a *cis*-vinyl species.

The fundamental point is that the face of the alkyne to which the proton binds defines the configuration of the vinyl species. Provided the carbon–carbon double bond is maintained upon the addition of the second proton the resulting alkene's configuration will be defined by the position of the initial protonation: *cis*-vinyl gives a *cis*-alkene and *trans*-vinyl gives a *trans*-alkene.

Clearly if the rates of the initial *exo* and *endo* protonations are sufficiently different then a stereoselective alkene will be formed, provided intermediate isomeric vinyl species or the isomeric coordinated alkenes do not equilibrate. Both isomeric vinyl and alkene complexes can equilibrate by protonation to form alkylidene ligands and alkyl ligands, respectively. Rapid rotation about the carbon–carbon single bond in either alkylidene or alkyl ligands prior to proton loss effectively destroys any selectivity (see Section 5.2). In order to avoid this problem the system must be carefully designed.

A question that must be addressed initially is: "Can protonation of a coordinated alkyne occur stereoselectively?" To answer this question the reaction of anhydrous HCl with the symmetrical alkyne PhCCPh bound to the symmetrical site $\{V(\eta^5\text{-}C_5H_5)_2\}$ has been studied [Eq. (27)].[49] The symmetrical nature

$$[V(\eta^5\text{-}C_5H_5)_2(\eta^2\text{-PhCCPh})] + 2HCl \longrightarrow [V(\eta^5\text{-}C_5H_5)_2Cl_2] + PhCHCHPh \quad (27)$$

of the entire system ensures that any stereoselectivity observed is a consequence of the rates of protonation and not of the ancillary ligands' "guiding" the proton preferentially to a particular face of the alkyne. Predominantly the *cis*-alkene (85%) is formed with 15% *trans* isomer.

The reaction exhibits a first-order dependence on the concentration of complex, but the dependence on the concentration of HCl is complicated (Fig. 10). This complicated acid dependence

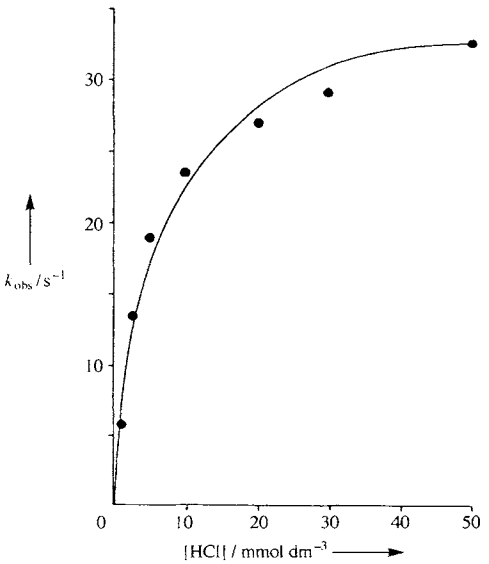

Fig. 10. Dependence of the observed rate constant k_{obs} on acid concentration for the protonation of $[V(\eta^5\text{-}C_5H_5)_2(\eta^2\text{-PhCCPh})]$.

mitigates against simple, direct proton attack at the coordinated alkyne, but rather indicates the mechanism depicted in Scheme 22 with the corresponding rate law shown in Equation (28).

$$k_{obs} = (k_2 + k_3K_1)[HCl]/(1 + K_1[HCl]) \quad (28)$$

The major pathway involves initial, rapid protonation of the metal to give $[VH(\eta^5\text{-}C_5H_5)_2(\eta^2\text{-PhCCPh})]^+$, followed by rate-limiting migration of the hydride to the alkyne necessarily producing the *cis*-vinyl species. In addition, protonation of the alkyne at the face remote from the metal produces the *trans*-vinyl species. Analysis of the data gives $(k_2 + k_3K_1) = 6.2 \times 10^3\ dm^3\,mol^{-1}\,s^{-1}$ and $K_1 = 1.56 \times 10^2\ dm^3\,mol^{-1}$. It seems likely that the carbon–carbon double bond of the vinyl ligand is retained throughout the second protonation, and hence the configuration of the final alkene is defined by the initial site of protonation of the coordinated alkyne.

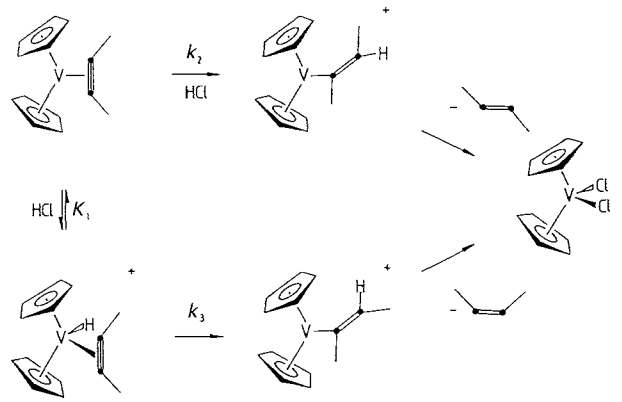

Scheme 22. Proposed mechanism for the protonation of the symmetrical complex $[V(\eta^5\text{-}C_5H_5)_2(\eta^2\text{-PhCCPh})]$.

Studies on $[Nb(\eta^5\text{-}C_5H_5)_2(CO)(CMeCHiPr)]$ show that protonation of the vinyl species gave an alkene of the same configuration as the vinyl ligand.[50] However, if the second protonation were to occur at the carbon atom remote from the metal, isomerization would result. Methylation of $[Nb(\eta^5\text{-}C_5H_5)_2(CO)(CMeCHiPr)]$ with $MeOSO_2F$ leads to an alkylidene species, which subsequently produces a mixture of alkene isomers (Scheme 23).

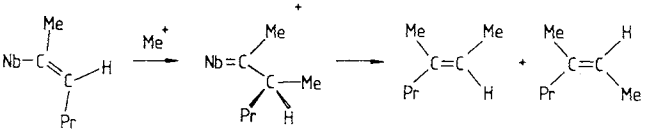

Scheme 23. Methylation of $[Nb(\eta^5\text{-}C_5H_5)_2(CO)(CMeCHiPr)]$ with $MeOSO_2F$ leading to a mixture of alkenes.

How then can we design the system so that the vinyl complexes do not protonate at the remote carbon atom and destroy the stereoselectivity? For protonation of vinyl complexes at either the metal or the remote carbon atom, a pair of electrons have to be supplied by the metal, and hence the formal oxidation state of the metal increases by two units. However, since $[V(\eta^5\text{-}C_5H_5)_2(PhCCHPh)]^+$ is a vanadium(IV) complex, protonation at the metal or remote carbon atom is impossible—it can only occur at the vanadium–carbon bond.

This illustrates a general way in which protonation of a complex can be controlled. Protonation of alkyne complexes where the oxidation state of the metal is less than four units from its maximum (that is, greater than +2 for V, Nb, or Ta; greater than +3 for Cr, Mo, or W, etc.) enforces the protonation of the derived vinyl species to occur at the carbon atom adjacent to the metal. In these circumstances, the configuration of the alkene product is always defined by that the vinyl species and hence by the kinetically favored site of protonation of the alkyne ligand.

Further quantitative analysis of the vanadium system in Equation (27) is possible. Since the isomeric alkene product distribution is defined by the rates of formation of the isomeric vinyl species the expression in Equation (29) can be derived,

$$\frac{[cis\text{-PhCHCHPh}]}{[cis\text{-PhCHCHPh}] + [trans\text{-PhCHCHPh}]} = \frac{k_3K_1}{k_3K_1 + k_2} \quad (29)$$

from which $k_2 = 9.3 \times 10^2\ dm^3 mol^{-1} s^{-1}$ and $k_3 = 33.8\ s^{-1}$. Since it can be estimated that $k_1 \geq 1 \times 10^6\ dm^3 mol^{-1} s^{-1}$, it is clear that the difference in the rates of protonation of the metal (to give *cis*-alkene) and alkyne (to give *trans*-alkene) would lead to essentially exclusive formation of *cis*-alkene. However, it is the relatively slow rate of intramolecular migration, together with the reversibility of the protonation at the metal that leads to the poorer stereoselectivity observed experimentally.

The reversibility of the initial protonation is another factor we have to consider in designing systems to give stereoselective alkenes. In certain circumstances, the initial site of protonation would not define the configuration of the product, for instance, if the initial protonation of the coordinated alkyne is reversible, or the favored isomeric vinyl species is protonated only slowly, whilst the minor isomeric vinyl complex protonates rapidly. However, this latter scenario seems unlikely since the isomeric vinyl species are necessarily only distinguished by the substituent on the carbon atom remote from the metal, and consequently one would expect that the rate of protonation of the carbon atom adjacent to the metal would be similar for the two isomers.

The stereoselectivity in $[V(\eta^5\text{-}C_5H_5)_2(\eta^2\text{-}PhCCPh)]$ is controlled entirely by the relative rates of protonation of the metal and the alkyne, and in this highly symmetrical complex the dominant product is the *cis*-alkene.

The nitrogenases specifically transform acetylene to *cis*-CHDCHD in vitro by a sequence of electron and proton transfer reactions.[51] Much speculation has centered around how the enzyme accomplishes this stereoselectivity.[7, 52] However, the results from this study indicate that the biological result needs little explanation: the enzyme is merely showing the normal stereoselectivity associated with this type of reaction.

In certain circumstances, stereoselective formation of alkenes by protonation of coordinated alkynes can also be accomplished under conditions of thermodynamic control. The reaction between anhydrous HX (X = Cl, Br, or BF_4) and complexes of the type *trans*-$[Mo(\eta^2\text{-alkyne})_2(dppe)_2]$ gives vinyl and alkylidyne complexes[53, 54] as shown by the examples in Equations (30) and (31), respectively. In both cases the overall stoichiometry

$$trans\text{-}[Mo(\eta^2\text{-}MeCCH)_2(dppe)_2] + HX \longrightarrow trans\text{-}[Mo(CHCHMe)X(dppe)_2] + MeCCH \quad (30)$$

$$trans\text{-}[Mo(\eta^2\text{-}MeCCH)_2(dppe)_2] + HX \longrightarrow trans\text{-}[Mo(CCH_2Me)X(dppe)_2] + MeCCH \quad (31)$$

requires the net addition of one molecule of HX, but clearly for the formation of the alkylidyne, a complex protonation/deprotonation pathway must operate. The mechanistic rationalization of how both types of products can be formed from the same reactants is shown in Scheme 24; the associated general rate law

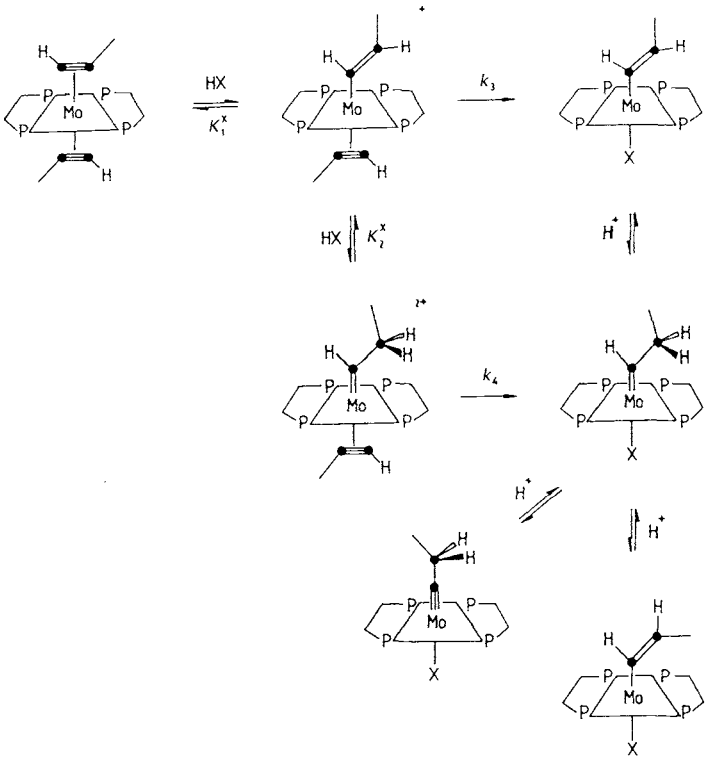

Scheme 24. Protonation of *trans*-$[Mo(\eta^2\text{-}MeCCH)_2(dppe)_2]$.

is given by Equation (32) if the dissociation of propyne is rate-limiting in both pathways.

$$k_{obs} = \frac{K_1^X[HX]\{k_3 + k_4 K_2^X[HX]\}}{1 + K_1^X[HX] + K_1^X K_2^X[HX]^2} \quad (32)$$

Initial, rapid protonation of *trans*-$[Mo(\eta^2\text{-}MeCCH)_2(dppe)_2]$ forms *trans*-$[Mo(CHCHMe)(\eta^2\text{-}MeCCH)(dppe)_2]^+$ ($K_1^{Cl} = 1.3 \times 10^2\ dm^3 mol^{-1}$) within 2 ms, which can be detected both by electronic spectroscopy and low temperature $^{31}P\{^1H\}$ NMR spectroscopy. Protonation of a propyne ligand decreases the electron density at the metal and consequently labilizes the *trans*-propyne to dissociation ($k_3 = 0.35\ s^{-1}$). Subsequent rapid binding of X^- at the site vacated by MeCCH gives the vinyl product, *trans*-$[MoX(CHCHMe)(dppe)_2]$, and at low concentrations of acid this is the exclusive product-forming pathway.

At high concentrations of acid, protonation of *trans*-$[Mo(CHCHMe)(\eta^2\text{-}MeCCH)(dppe)_2]^+$ to form *trans*-$[Mo(CHCH_2Me)(\eta^2\text{-}MeCCH)(dppe)_2]^{2+}$ can occur ($K_2^{Cl} = 3.0\ dm^3 mol^{-1}$) before dissociation of the propyne ligand. This second protonation further labilizes the *trans*-propyne ligand ($k_4 = 2.58\ s^{-1}$), which is lost in the rate-limiting step. Rapid attack by X^- and proton release from the alkylidene ligand gives either *trans*-$[Mo(CHCHMe)X(dppe)_2]$ (proton loss from the remote carbon atom) or *trans*-$[Mo(CCH_2Me)X(dppe)_2]$ (proton loss from the adjacent carbon atom).

An important mechanistic conclusion is that the product of the reaction (vinyl or alkylidyne complex) is not defined by the site of protonation but is decided by factors that have their influence after the rate-limiting step. Although the alkylidyne species has only been isolated in the reaction with $HBF_4 \cdot OEt_2$,

it seems likely that, irrespective of the acid, the equilibrium mixture of isomeric vinyl complexes, alkylidene, and alkylidyne species shown on the right-hand side of Scheme 24 is present in solution. Which product is actually isolated will depend on the magnitude of the equilibrium constants interconnecting these species, or merely the relative solubilities. It is unlikely that a fluoro ligand favors proton loss from the adjacent carbon atom whilst the chloro or bromo ligand favors proton loss from the remote carbon atom. Rather it seems more likely that the least soluble is product isolated.

The mechanism shown in Scheme 24 has important consequences for the configuration of the vinyl ligand. Irrespective of the initial site of protonation and the resulting configuration of the vinyl ligand in *trans*-[Mo(CHCHMe)(η^2-MeCCH)(dppe)$_2$]$^+$, at high concentrations of acid the reaction proceeds via the alkylidene intermediate *trans*-[Mo(CHCH$_2$Me)(η^2-MeCCH)(dppe)$_2$]$^{2+}$. Free rotation around the carbon–carbon single bond in this intermediate prior to proton loss means that any stereoselectivity introduced at the initial protonation is destroyed. However, *trans*-[Mo(CHCHMe)Br(dppe)$_2$] isolated from this reaction shows partially resolved peaks in the ^{1}H NMR spectrum, which are attributable to the vinyl ligand. Thus, the resonance at $\delta = 10.9$ is a doublet ($J_{H,H} = 8.8$ Hz), and the resonance at $\delta = 9.5$ is a multiplet. In addition the methyl signal at $\delta = 1.15$ is a doublet ($J_{H,H} = 5$ Hz). These coupling constants are consistent with a *cis*-vinyl ligand ($J^{cis}_{H,H} = 6-14$ Hz, $J^{trans}_{H,H} = 11-20$ Hz). Clearly this stereoselective formation of the *cis*-vinyl species cannot reflect a kinetic preference, but must be a consequence of a signifiant difference in the thermodynamic stability or solubility between *trans*-[Mo(*cis*-CHCHMe)Br(dppe)$_2$] and *trans*-[Mo(*trans*-CHCHMe)Br(dppe)$_2$]. That is, the stereoselectivity is thermodynamically controlled.

Thus, at least in principle, stereoselective formation of an alkene by protonation of a coordinated alkyne can be accomplished by thermodynamic control. Protonation of a particular configuration of a vinyl ligand at the carbon remote from the metal generates an alkylidene species, and subsequent deprotonation produces an equilibrium mixture of *cis* and *trans* vinyl species. Further protonation of this mixture will often result in a mixture of isomeric alkenes. However, a specific configuration of an alkene can be produced provided 1) there is a significant difference in the thermodynamic stabilities of the isomeric vinyl species and 2) protonation of the vinyl species to give the alkene is significantly slower than the rate of proton equilibration between the vinyl and alkylidene species.

It is worthwhile just briefly considering the factors that result in a significant difference in the thermodynamic stabilities of the isomeric vinyl species. Clearly the major contributors must be the size of both the vinyl substituent and the coligands of the metal. If both are bulky, one can be reasonably confident that the *trans*-vinyl residue, minimizing unfavorable steric interactions, would be the more stable thermodynamically. However, in the study on *trans*-[Mo(η^2-MeCCH)$_2$(dppe)$_2$] (with a methyl substituent) the *cis*-vinyl ligand is preferred, probably because the methyl group is buried in the surrounding coligand framework.

Finally, it should be noted that thermodynamic control of stereochemistry can only operate with alkynes other than acetylene, since the differentiation in stabilities is exclusively a consequence of the substituent on the vinyl ligand.

6. Summary and Outlook

In this review I have highlighted the mechanistic aspects associated with the protonation of unsaturated hydrocarbon residues bound to transition metal sites and emphasized how this reactivity is a natural consequence of having two sites on the same molecule that undergo slow proton transfer reactions. Three key mechanistic principles emerge with which the reactivity of these systems can be understood. 1) Protonation can occur at either the metal or the hydrocarbon ligand. 2) The initial site of attack may not be the final residence of the proton. 3) Transfer of the proton between metal and ligand can occur by intramolecular or acid-catalyzed pathways.

These principles have some important repercussions, the most fundamental of which is that protonation of complexes containing unsaturated hydrocarbons is invariably more complicated than would be imagined from inspection of the structures of the products. Consequently, a reaction can be stoichiometrically regioselective in that the product is ultimately protonated at a single site, though mechanistically the reaction might proceed by several pathways in which the complex is initially protonated at different sites.

An overall picture of the hydrocarbon-evolving transformations discussed in this article is shown in Scheme 25. This dia-

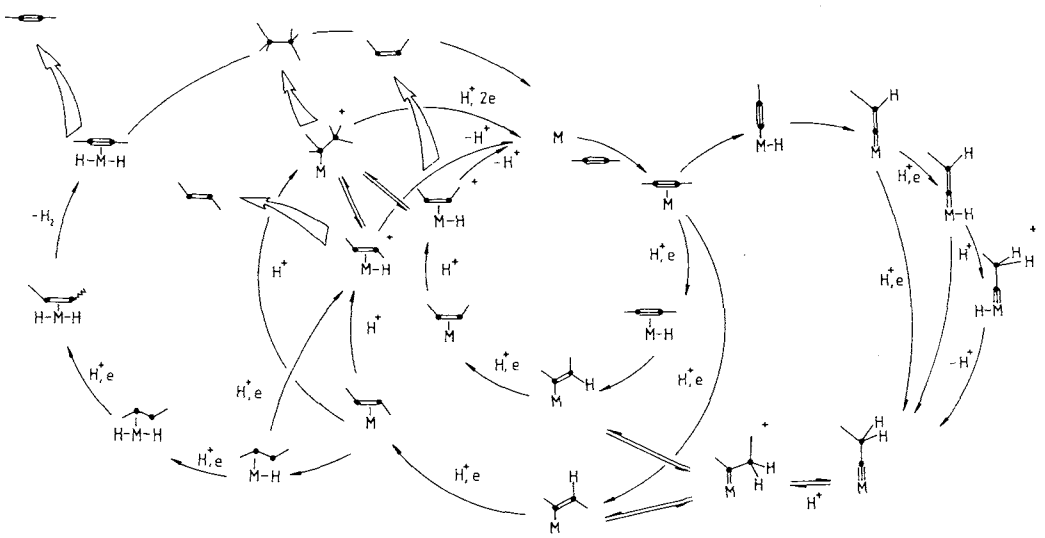

Scheme 25. Overview of all the transformations discussed in this review in which hydrocarbon ligands are released.

gram illustrates how the competitive protonation of metal and ligand can be exploited, first to control the products of the reaction and second, to control the stereochemistry of the products.

The future is still intellectually demanding. Although a lot of synthetic chemistry has resulted in a general understanding of which site is the ultimate residence of the proton, we are still a long way from understanding the mechanistic factors that discriminate between initial protonation of the metal and the hydrocarbon residue. Only if we can understand the kinetic features of this type of reaction can we hope to design complexes whose reactivity and reaction products can be defined prior to their preparation.

Finally, what about catalysis? The diagram in Scheme 25 indicates several cyclic processes established by piecing together the stoichiometric reactions discussed in this article. A feature of all the reactions discussed herein is the formation of well-defined metal-containing products. For instance, $[MoH_2Cl_2(dppe)_2]$ has been isolated from the reaction of HCl with *trans*-$[MoH(\eta^3\text{-}C_3H_5)(dppe)_2]$. In a sense, $[MoH_2Cl_2(dppe)_2]$ is "exhausted" since it has supplied electrons to protons, either to form hydride ligands or evolve dihydrogen. However, $[MoH_2Cl_2(dppe)_2]$ can be reduced under an atmosphere of propene to form *trans*-$[MoH(\eta^3\text{-}C_3H_5)(dppe)_2]$,[42] and hence, in principle, we have a catalyst, and a versatile catalyst at that, since by changing the concentration of acid used at each turnover we could selectively produce propene or propyne. Similarly, we can envisage a catalyst that selectively produces ethane or ethene based on *trans*-$[Mo(\eta^2\text{-}C_2H_4)_2(dppe)_2]$. However, in practice, there is a problem in adapting these systems to be truly catalytic because of the preferential reduction of protons to dihydrogen in any system containing an acid and a reductant. A major target in the near future must be finding solutions to this problem. After all, if nature can find ways of minimizing proton reduction in the conversion of acetylene into ethene or ethane by the nitrogenases, so can chemists!

Received: June 16, 1995 [A 119 IE]
German version: *Angew. Chem.* **1996**, *108*, 1024 - 1046

[1] R. A. Henderson, *J. Chem. Soc. Dalton Trans.* **1995**, 503, and references therein.
[2] P. G. Leuhert, *Proc. R. Soc. London A* **1968**, *303*, 45.
[3] P. J. Toscano, L. G. Marzilli, *Prog. Inorg. Chem.* **1984**, *31*, 105, and references therein.
[4] D. Qui, M. Kumar, S. W. Raysdale, T. G. Spiro, *Science* **1994**, *264*, 817.
[5] A. C. Rosenzweig, S. J. Lippard, *Acc. Chem. Res.* **1994**, *27*, 229.
[6] L. Que, Jr. in *Bioinorganic Catalysis* (Ed.: J. Reedijk), Marcel Dekker New York, **1993**, p. 347, and references therein.
[7] D. J. Evans, R. A. Henderson, B. E. Smith in *Bioinorganic Catalysis* (Ed.: J. Reedijk), Marcel Dekker, New York, **1993**, p. 89, and references therein.
[8] M. Eigen, *Angew. Chem.* **1963**, *75*, 489; *Angew. Chem. Int. Ed. Engl.* **1964**, *3*, 1, and references therein.
[9] R. P. Bell, *The Proton in Chemistry*, 2nd ed., Chapman and Hall, London, **1973**.
[10] K. W. Kramarz, J. R. Norton, *Prog. Inorg. Chem.* **1994**, *42*, 1.
[11] R. P. Bell, R. G. Pearson, *J. Chem. Soc.* **1953**, 3443.
[12] Ref. [9], p. 213.
[13] R. P. Bell, *Acids and Bases: Their Quantitative Behaviour*, Chapman and Hall, London, **1971**, p. 71.
[14] R. P. Bell, B. G. Cox, *J. Chem. Soc. B* **1971**, 654.
[15] R. F. Jordan, J. R. Norton, *ACS Symp. Ser.* **1982**, *198*, 403, and references therein.
[16] S. S. Krisiánsdóttir, A. J. Loendorf, J. R. Norton, *Inorg. Chem.* **1991**, *30*, 4470, and references therein.
[17] G. Cerichelli, G. Illuminati, G. Ortaggi, A. M. Giuliani, *J. Organomet. Chem.* **1977**, *127*, 357, and references therein.
[18] M. I. Bruce, A. G. Swincer, *Adv. Organomet. Chem.* **1983**, *22*, 59, and references therein.
[19] K. R. Birdwhistell, S. J. N. Burgmayer, J. L. Templeton, *J. Am. Chem. Soc.* **1985**, *107*, 4474, and references therein.
[20] R. M. Bullock, *J. Am. Chem. Soc.* **1987**, *109*, 8087.
[21] N. M. Kostic, R. F. Fenske, *Organometallics* **1982**, *1*, 974.
[22] A. Mayr, K. C. Shaefer, H. C. Huang, *J. Am. Chem. Soc.* **1984**, *106*, 1517, and references therein.
[23] A. J. L. Pombeiro, A. Hills, D. L. Hughes, R. L. Richards, *J. Organomet. Chem.* **1988**, *352*, C5.
[24] M. F. N. N. Carvalho, R. A. Henderson, A. J. L. Pombeiro, R. L. Richards, *J. Chem. Soc. Chem. Comm.* **1989**, 1796.
[25] S. J. Holmes, R. R. Schrock, *J. Am. Chem. Soc.* **1981**, *103*, 4599.
[26] N. M. Kostic, R. F. Fenske, *J. Am. Chem. Soc.* **1981**, *103*, 4677.
[27] M. Green, A. G. Orpen, I. D. Williams, *J. Chem. Soc. Chem. Comm.* **1982**, 493, and references therein.
[28] A. Mayr, C. M. Bastos, *J. Am. Chem. Soc.* **1990**, *112*, 7797.
[29] J. H. Freudenberger, R. R. Schrock, *Organometallics* **1985**, *4*, 1937.
[30] C. Roger, G. S. Bodner, W. G. Hatton, J. A. Gladysz, *Organometallics* **1991**, *10*, 3266, and references therein.
[31] D. L. Hughes, A. J. L. Pombeiro, C. J. Pickett, R. L. Richards, *J. Chem. Soc. Chem. Comm.* **1984**, 992.
[32] A. J. L. Pombeiro, D. L. Hughes, R. L. Richards, J. Silvestre, R. Hoffmann, *J. Chem. Soc. Chem. Comm.* **1986**, 1125.
[33] R. A. Henderson, A. J. L. Pombeiro, R. L. Richards, Y. Wang, *J. Organomet. Chem.* **1993**, *447*, C11.
[34] R. A. Henderson, K. E. Oglieve, *J. Chem. Soc. Chem. Comm.* **1991**, 584, and references therein.
[35] K. E. Oglieve, R. A. Henderson, *J. Chem. Soc. Dalton Trans.* **1991**, 3295, and references therein.
[36] J. W. Byrne, H. U. Blaser, J. A. Osborne, *J. Am. Chem. Soc.* **1975**, *97*, 3871.
[37] M. L. H. Green, L. L. Wong, *J. Chem. Soc. Chem. Comm.* **1988**, 677, and references therein.
[38] J. Halpern, L. Cai, P. J. Desrosiers, Z. Lim, *J. Chem. Soc. Dalton Trans.* **1991**, 717.
[39] T. Al-Salih, C. J. Pickett, *J. Chem. Soc. Dalton Trans.* **1985**, 1255.
[40] R. A. Henderson, D. L. Hughes, K. E. Oglieve, unpublished.
[41] K. E. Oglieve, R. A. Henderson, *J. Chem. Soc. Chem. Comm.* **1993**, 474.
[42] R. A. Henderson, K. E. Oglieve, unpublished.
[43] R. A. Henderson, K. E. Oglieve, *J. Chem. Soc. Dalton Trans.* **1994**, 767.
[44] C. P. Casey, C. S. Yi, *Organometallics* **1991**, *10*, 33.
[45] T. H. Whitesides, J. P. Neilan, *J. Am. Chem. Soc.* **1975**, *97*, 907.
[46] G. K. Turner, W. Kläui, M. Scotti, H. Werner, *J. Organomet. Chem.* **1975**, *102*, C9.
[47] U. T. Mueller-Westerhoff, T. J. Haas, G. F. Swiegers, T. K. Leipert, *J. Organomet. Chem.* **1994**, *472*, 229, and references therein.
[48] A. Bond, M. Green, S. H. Taylor, *J. Chem. Soc. Chem. Comm.* **1973**, 112.
[49] R. A. Henderson, D. J. Lowe, P. Salisbury, *J. Organomet. Chem.* **1995**, *489*, C22.
[50] J. A. Labinger, J. Schwartz, *J. Am. Chem. Soc.* **1975**, *97*, 1596.
[51] M. J. Dilworth, R. R. Eady, M. E. Eldridge, *Biochem. J.* **1988**, *249*, 745.
[52] G. A. Ashby, M. J. Dilworth, R. N. F. Thorneley, *Biochem. J.* **1987**, *247*, 547.
[53] A. Hills, D. L. Hughes, N. Kashef, M. A. N. D. A. Lemos, A. J. L. Pombeiro, R. L. Richards, *J. Chem. Soc. Dalton Trans.* **1992**, 1775, and references therein.
[54] R. A. Henderson, K. E. Oglieve, P. Salisbury, *J. Ghem. Soc. Dalton Trans.*, **1995**, 2479.